

ISSN 2449-8955
EJBRAT 8(1) 2018

Volume 8
Number 1
January-March 2018

European Journal of Biological Research

MNiSW points 2017: **11**
Index Copernicus 2017: **100**

<http://www.journals.tmkarpinski.com/index.php/ejbr>
e-mails: ejbr@tmkarpinski.lh.pl ejbr@interia.eu

European Journal of Biological Research

ISSN 2449-8955

Editor-in-Chief

Tomasz M. Karpiński
*Poznań University of Medical Sciences, Poznań,
Poland*

Co-Editor

Artur Adamczak
*Institute of Natural Fibres and Medicinal Plants,
Poznań, Poland*

Editorial Secretary

Joanna Bródka, *Poznań, Poland*

Statistical Editor

Paweł Zaprawa, *Lublin, Poland*

Language Editor

Jan Nowacki, *London, UK*

Scientific Editorial Board

Tamara Bayanova, *Apatity, Russia*
Payam Behzadi, *Tehran, Iran*
Alexander Ereskovsky, *Marseille, France*
Agnieszka Gałuszka, *Kielce, Poland*
Vittorio Gentile, *Naples, Italy*
Stanisław Hałas, *Lublin, Poland*
Fadi Hage Chehade, *Beirut, Lebanon*
Afaf M. Hamada, *Stockholm, Sweden*
Sven Herzog, *Tharandt, Germany*
Liviu Holonec, *Cluj-Napoca, Romania*
Miłosz A. Huber, *Lublin, Poland*
Shri Mohan Jain, *Helsinki, Finland*
Wouter Kalle, *Wagga Wagga, Australia*
Tomasz Klepka, *Lublin, Poland*
Nikolaos Labrou, *Athens, Greece*
Igor Loskutov, *Sankt Petersburg, Russia*
Ákos Máthé, *Sopron, Hungary*
Ahmed El-Mekabaty, *Mansoura, Egypt*
Artem V. Mokrushin, *Apatity, Russia*
Shahid M. Mukhtar, *Birmingham, USA*
Robert Pal, *Pécs, Hungary*
Amal K. Paul, *Kolkata, India*
Rajiv Ranjan, *Narkatia Ganj, India*
Antonio Tiezzi, *Viterbo, Italy*
Timotej Verbovšek, *Ljubljana, Slovenia*
Vladimir K. Zhironov, *Apatity, Russia*

List of Peer-Reviewers <http://www.journals.tmkarpinski.com/index.php/ejbr/pages/view/reviewers>

Author Guidelines <http://www.journals.tmkarpinski.com/index.php/ejbr/about/submissions>

More information www.journals.tmkarpinski.com/index.php/ejbr

DISCLAIMER

The Publisher and Editors cannot be held responsible for errors and any consequences arising from the use of information contained in this journal; the views and opinions expressed do not necessarily reflect those of the Publisher and Editors, neither does the publication of advertisements constitute any endorsement by the Publisher and Editors of the products advertised.

Cover: <http://openwalls.com/image?id=20115>, Licence Creative Commons Attribution 3.0 Unported (CC BY 3.0)

Copyright: © The Author(s) 2018. European Journal of Biological Research © 2018 T.M.Karpiński. All articles and abstracts are open-access, distributed under the terms of the Creative Commons Attribution Non-Commercial 4.0 International License, which permits unrestricted, non-commercial use, distribution and reproduction in any medium, provided the work is properly cited.

Publisher and Editor's office: Tomasz M. Karpiński, Szkółkarska 88B, 62-002 Suchy Las, Poland, e-mail: ejbr@interia.eu

Contents

- 1-6 **Petrified *Geobacillus thermoglucosidasius* colony to strontianite**
Naoto Yoshida, Rie Murai, Keiji Kiyoshi
- 7-13 **Effects of cobalt and manganese on biomass and nitrogen fixation yields of a free-living nitrogen fixer - *Azotobacter chroococcum***
Justina Orji, Chima Ngumah, Hanna Asor, Anulika Anuonyemere
- 14-20 ***Neurospora tetraspora* D. Garcia, Stchigel & Guarro (= *Gelasinospora tetrasperma* Dowding) as a first record to Egypt**
A. H. Moubasher, M. A. Abdel-Sater, Zeinab Soliman
- 21-25 **The relevance of sebum composition in the etiopathogeny of acne**
Marisa Gonzaga da Cunha, Francisca Daza, Carlos D. Aparecida Machado Filho, Glaucia Luciano da Veiga, Fernando Fonseca
- 26-33 **Antioxidant potential of the farmer preferred selections of *Solanum aethiopicum* vegetable consumed in central Uganda**
S. Sekulya, A. Nandutu, A. Namutebi, J. Ssozi, M. Masanza, B. Kabod, J. N. Jagwe, A. Kasharu, D. Rees, E. B. Kizito
- 34-41 **Comparative stem anatomy of four taxa of Calycanthaceae Lindl.**
Niroj Paudel, Kweon Heo

Petrified *Geobacillus thermoglucosidasius* colony to strontianite

Naoto Yoshida*, Rie Murai, Keiji Kiyoshi

Department of Biochemistry and Applied Biosciences, University of Miyazaki, 1-1 Gakuen Kibanadai-Nishi, Miyazaki 889-2192, Japan

*Corresponding author: Naoto Yoshida; E-mail: a04109u@cc.miyazaki-u.ac.jp

Received: 20 November 2017; Revised submission: 09 January 2018; Accepted: 12 January 2018

Copyright: © The Author(s) 2018. European Journal of Biological Research © T.M.Karpiński 2018. This is an open access article licensed under the terms of the Creative Commons Attribution Non-Commercial 4.0 International License, which permits unrestricted, non-commercial use, distribution and reproduction in any medium, provided the work is properly cited.

DOI: <http://dx.doi.org/10.5281/zenodo.1146702>

ABSTRACT

When biomass of the thermophilic bacteria *Geobacillus thermoglucosidasius* is brought into contact with a hydrogel containing sodium acetate and strontium, the biomass petrifies and hardens, becoming a mineralized thin film after incubation at 60°C for 72 h. Analysis by energy dispersive X-ray and X-ray diffraction shows that the mineralized thin film is strontianite. This is the first report of biomass completely changing to strontianite. Strontianite of thermophilic bacterial origin may be formed in the hydrothermal oligotrophic environment of the deep subsurface.

Keywords: *Geobacillus*; Thermophilic bacterium; Biomineralization; Strontianite; Mineralized thin film.

1. INTRODUCTION

Strontianite was first discovered in 1787, in the heavy, white stone produced by the town of Strontian in Argyll, Scotland, United Kingdom [1]. Sir Humphry Davy subsequently discovered the element strontium in this mineral in 1808 [2]. Strontianite is actually a rare carbonate mineral, and along with celestine, it is one of the few minerals containing strontium.

To date, we have made various contributions toward clarification of the mechanisms of bacterial calcite formation and the industrial applications of calcite [3, 4]. The major contributions have been the discovery that thermophilic bacteria catalyze the formation of calcite monocrystals at 60°C, and the discovery of a definite, reproducible method for forming calcite crystals with a matrix of hydrogels containing a lower fatty acid salt and calcium. This is a new method, whereby thermophilic bacteria biomass is brought into contact with a hydrogel, causing it to form crystals. Results to date have shown that if fresh *Geobacillus thermoglucosidasius* biomass is placed on agar gel containing carboxylates of up to 4C and calcium ions, and is incubated at 60°C, numerous calcite monocrystals of major axis length in the region of 100 µm form within the biomass. *G. thermoglucosidasius* does not catalyze crystal formation if the calcium is replaced by beryllium or magnesium, which are members of the same family. In the present paper, we present a new phenomenon whereby the whole biomass of the thermophile *G. thermoglucosidasius* is petrified if its biomass is placed on agar gel containing strontium, a member of the same family as calcium, and we conjecture that the mineral is strontianite, which is rare in the natural world.

2. MATERIALS AND METHODS

2.1. Preparation and observation of mineralized thin film

In order to obtain fresh biomass, *G. thermoglucosidasius* was seeded onto soytone-casein digest (SCD) agar culture medium and cultivated for 18 h at 60°C. Fresh *G. thermoglucosidasius* biomass (wet weight, 10–20 mg) was scraped off with a loop and applied to the surface of agar gel containing

7 mM strontium chloride and 25 mM sodium acetate (crystal forming gel) so that it formed a circle approx. 1 cm in diameter (Fig. 1). This was incubated for 72 h at 60°C. Changes in the biomass applied to the crystal forming gel were observed using a SZX-ILLK100 stereoscopic microscope (Olympus Corporation, Tokyo, Japan). Monocrystals were observed using a scanning electron microscope in accordance with the customary protocols [4].

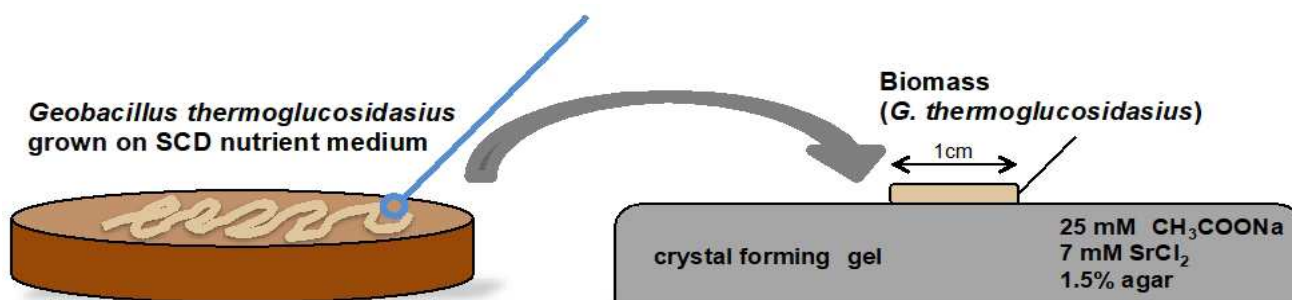


Figure 1. Method for converting *Geobacillus thermoglucosidasius* biomass into mineralized thin film. The method is simply to apply 10–20 mg of cells of *G. thermoglucosidasius* cultured on SCD medium to the surface of agar gel in a circle 1 cm across, and maintain them at 60°C for 72 h. The biomass petrifies, becoming a mineralized thin film.

2.2. Energy dispersive X-ray elemental analysis of mineralized thin film

The elemental composition of the mineralized thin film was investigated using an energy dispersive X-ray (EDX) analysis device (EMAX-5770; Horiba, Ltd.). Analyses were carried out at an accelerating voltage (tube voltage) of 20.0 kV and a probe current of 0.26 nA. Strontium carbonate (Wako Pure Chemical Industries, Ltd.) was used as the reference spectrum.

2.3. Powder X-ray diffraction analysis of mineralized thin film

Powder X-ray diffraction analysis of mineralized thin film was carried out using a PW3050/65 powder X-ray diffractometer (PANalytical) fitted with a copper rotary anticathode, a graphite-monochromator, a scintillation counter, and a rotary sample stage. Analyses were carried out according to the Bragg-Brentano method, at an output voltage of 45 kV and 40 mA, with a divergence slit of 0.87°

and a receiving slit of 0.1 mm. Scanning regions of the diffraction angle (2θ) were 10°–90° at a step interval of 0.025°, and the scanning rate was 4.0°/min. The mineralized thin film was ground into powder in a microtube and was placed on a sample stage. The reference spectrum was obtained from strontium carbonate (Wako Pure Chemical Industries, Ltd.). The waveform of the thin mineralized film spectrum was compared to the International Centre for Diffraction Data (ICDD) database for identification.

2.4. Energy dispersive X-ray elemental analysis of mineral crystals prepared on gel containing mixed calcium and strontium

G. thermoglucosidasius was seeded onto soytone-casein digest (SCD) agar culture medium and cultivated for 18 h at 60°C. Fresh *G. thermoglucosidasius* biomass (wet weight 10–20 mg) was scraped off with a loop and applied to the surface of agar gel containing strontium chloride, calcium chloride, and 25 mM sodium acetate (crystal for-

ming gel) so that it formed a circle approx. 1 cm in diameter. Concentrations of calcium and strontium in the agar gel were combined as follows; with calcium concentrations of 0, 1, 2, 3, 4, 5, 6, and 7 mM, the respective strontium concentrations were 7, 6, 5, 4, 3, 2, 1, and 0 mM. The culture was incubated for 72 h at 60°C. The mineral that formed was prepared according to conventional protocols [3], and energy dispersive X-ray (EDX) elemental analysis was performed.

2.5. Inductively coupled plasma (ICP) atomic emission spectroscopy

Samples of 5-10 g of the mineral crystals that had formed on crystal forming gel containing strontium and calcium in different proportions was completely dissolved in 1N hydrochloric acid and made up to a final volume of 25 ml with pure water. The elemental composition of each of these solutions was analyzed by inductively coupled plasma atomic emission spectroscopy using an ICPS-8100 emission spectrometer (Shimadzu Corporation).

3. RESULTS AND DISCUSSION

3.1. Preparation and observation of mineralized thin film

The biomass applied to the crystal forming gel was a *G. thermoglucosidasius* colony, and immediately following application to the gel, it had a fresh luster (Fig. 2A). After incubation for 7 h at 60°C, many well shaped globular monocrystals 20-50 µm in size had appeared in the biomass (Fig. 3). The number of monocrystals in the biomass increased with time, and they began to form clusters that adhered to one another. After 72 h, the biomass on top of the crystal forming gel was covered by mineral crystals, so that the biomass in its entirety was petrified with its shape intact (Fig. 2B). The petrified biomass was strong and could easily be pulled off the surface of the crystal forming gel (Fig. 2C). A magnified image shows that the petrified bacteria are a thin film formed of globular monocrystals massed together (Fig. 2D). The thickness of the thin film is 20-50 µm. All lumps of biomass appear to have been replaced by hard, inorganic mineral.

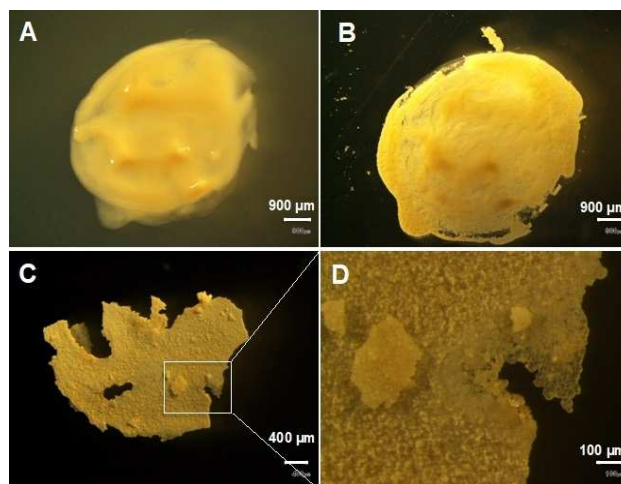


Figure 2. Petrification of *Geobacillus thermoglucosidasius* biomass on solidified agar containing 25 mM sodium acetate, and 7 mM strontium chloride. *G. thermoglucosidasius* biomass was placed onto the agar surface (A). After incubation at 60°C for 72 h, biomass transformed to mineralized thin film (B). Mineralized thin film could be isolated from the agar surface (C). Magnified observation indicated that the mineralized thin film consisted of numerous spherical crystals (D).

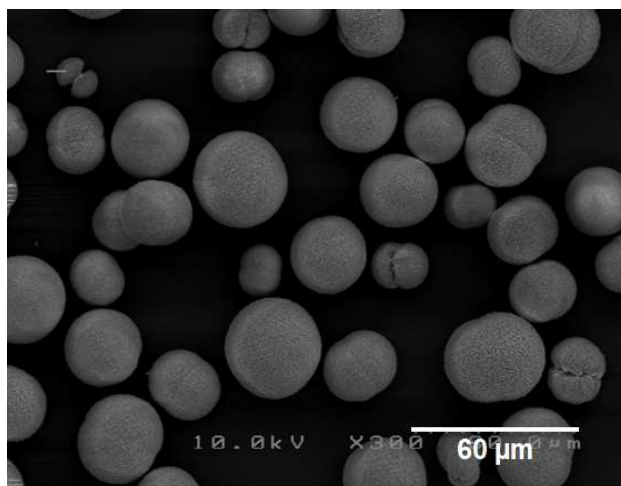


Figure 3. Scanning electron microscope observation of monocrystals of strontianite formed in the biomass of *G. thermoglucosidasius*.

The mineralized thin film was incubated for 48 h at 100°C to dry it completely, and when it was then burned with a Bunsen burner, the weight decreased to 84.8% of its previous weight. From this, it appears that 15.2% by weight of the mineralized thin film comprises organic or volatile material. We conjecture that *G. thermoglucosidasius* cells or spores are embedded within the mineralized thin film.

3.2. Energy dispersive X-ray elemental analysis of the mineralized thin film

EDX analysis shows that the spectrum obtained from the mineralized thin film closely resembles the spectrum obtained from pure strontium carbonate (Fig. 4). The analysis showed that if the ratio of strontium atoms in strontium carbonate is taken as 100, this ratio in the mineralized thin film is 94 and the film contains 6% (atm%) calcium atoms. If the oxygen and carbon are excluded, the elemental composition is strontium with a very small quantity of calcium. Strontium and calcium belong to the same family, so they exhibit very similar behavior as elements. As the crystal forming gel did not contain calcium, the calcium contained in the mineralized thin film probably came from calcium that was already present in the thermophilic bacteria.

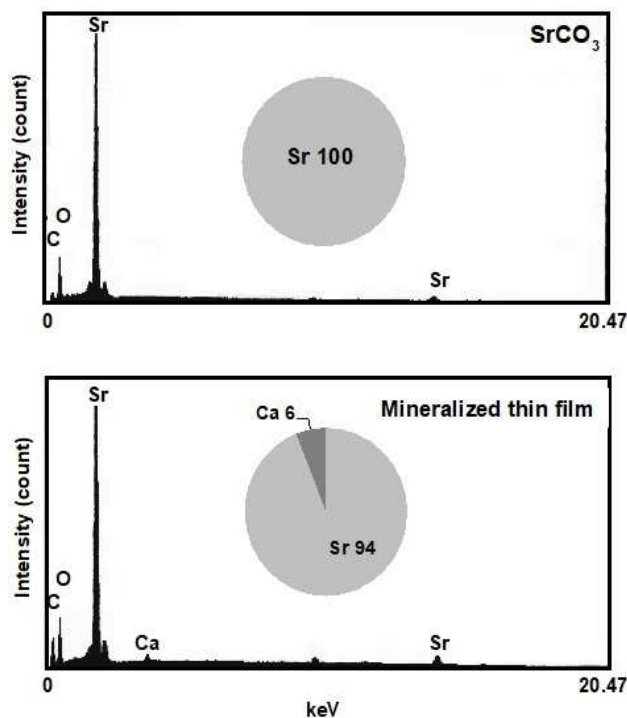


Figure 4. Energy Dispersion X-ray (EDX) spectrum of referenced purified strontium carbonate and mineralized thin film. The pie charts show the elemental composition proportions with carbon and oxygen excluded. Strontium accounts for 100% of strontium carbonate, but the mineralized thin film is composed of 94% strontium and 6% calcium.

3.3. Powder X-ray diffraction analysis of the mineralized thin film

The mineralized thin film was powdered and analyzed by powder X-ray diffraction, the results showing that the spectrum of the mineralized thin film was similar to that of pure strontium carbonate (Fig. 5). When the waveform of the spectrum was checked against the ICDD database, the thin film was identified as strontianite.

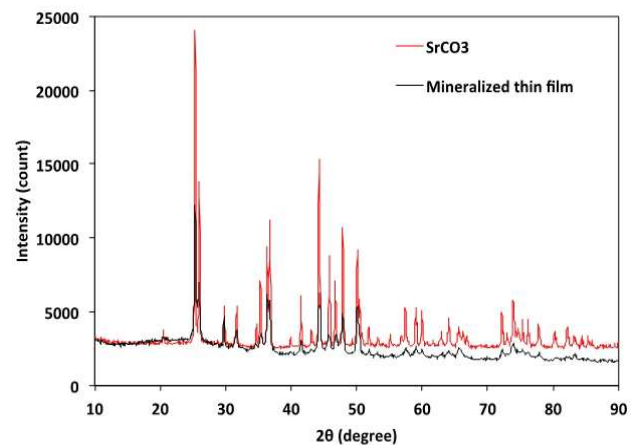


Figure 5. Powder X-ray diffraction patterns of referenced purified strontium carbonate and mineralized thin film.

3.4. Energy dispersive X-ray elemental analysis of mineral crystals prepared on gel containing mixed calcium and strontium

In order to investigate the elemental composition of the mineral that formed on mixed calcium and strontium gels, EDX analysis was performed on mineral that formed on gels containing different proportions of strontium chloride and sodium chloride (Fig. 6). A strontianite thin film containing 6% calcium formed on crystal forming gel containing only 7 mM strontium. When the gel contained mixed calcium and strontium, there was no thin film formation, and instead, a grain-shaped mineral formed. As the proportion of calcium in the gel increased gradually, the proportion of calcium in the mineral also increased. When the concentration in the gel was 3 mM calcium and 4 mM strontium, the ratio of calcium atoms to strontium atoms in the mineral was roughly 3:4. Similarly, when the concentration in the gel was 6 mM calcium and

1 mM strontium, the ratio of calcium atoms to strontium atoms in the mineral was roughly 6:1. Thus, the ratio of strontium to calcium in the mineral roughly agreed with the ratio of the two elements in the crystal forming gel. However, in the gel containing only 7 mM calcium, magnesium calcite containing 6% magnesium formed. This mineral has previously been shown to be magnesium calcite by XRD analysis [3].

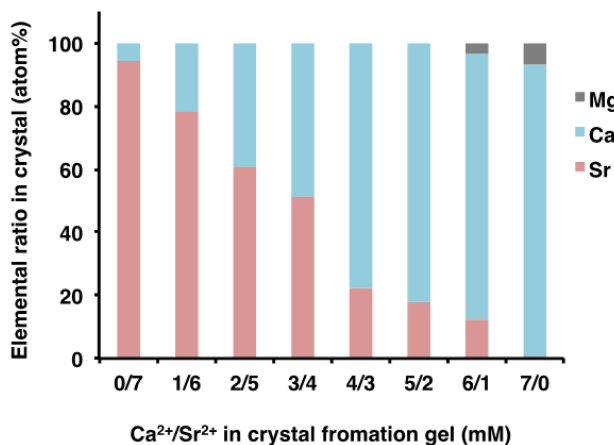


Figure 6. Elemental ratio in mineralized thin film and biominerals formed in *G. thermoglucosidasius* biomass on agar gel containing different Ca²⁺/Sr²⁺ ratio.

3.5. Elemental analysis of mineral crystals by inductively coupled plasma (ICP)

Elemental composition analysis by EDX is able to show the elemental composition of the surface of a material, but is unable to reveal the elemental composition inside the material. We therefore, used ICP to analyze the elemental composition of the mineral that formed on crystal forming gel containing strontium and calcium in different proportions. With gel containing 7 mM calcium and 6 mM strontium, the ratio of calcium atoms to strontium atoms in the mineral was roughly 7:6. Similarly, with gel containing 7 mM calcium and 10 mM strontium, the ratio of calcium atoms to strontium atoms in the mineral was roughly 7:10. Thus, as with EDX analysis, ICP elemental analysis showed that the ratio of calcium and strontium in the mineral roughly agreed with the ratio of the two elements in the crystal forming gel. These experimental results show that a shift from

strontianite to calcite can occur readily. The ease with which strontium and calcium are incorporated into the carbonate mineral is reflected in the concentration ratios. By following the present method for forming crystals, intermediate carbonate minerals between strontianite and calcite can easily be formed.

Carbonate minerals containing strontium and calcium in various different ratios can be found in nature [5, 6]. Strontium is a soft, silvery-white metal present in the Earth's crust at a mean concentration of about 370 ppm (0.037%) [7]. In the deep subsurface there is great geothermal heat, and it can easily be assumed that the temperature reaches 60°C at just a few kilometers underground [8, 9]. Wellsbury et al. [10] subjected organic matter from marine sediments to thermal decomposition at about 10-60°C, and they showed that this matter changed to acetic acid. Gold [11, 12] argues the existence of a biosphere in the deep subsurface of the Earth. Acetogenic bacteria discovered in the deep subsurface are known to produce acetic acid through anaerobic respiration [13, 14]. In addition, thermophilic acetogenic bacteria that live at 60°C have been isolated [15, 16]. It therefore, seems clear that lower fatty acids, such as acetic acid, are present in the deep subsurface of the Earth [17, 18]. If *G. thermoglucosidasius* (biofilm) at 60°C in the deep subsurface were to encounter acetic acid made by acetogenic bacteria and thermophilic acetogenic bacteria, and also strontium ions in groundwater, it would surely catalyze the formation of strontianite [19]. The elaboration of these exocellular strontianite formations enables the organism in biofilm to regulate its strontium content. The role of exocellular biomineralization may be concerned with processes of ion regulation and detoxification of heavy metal. The strontianite produced within the Earth [20] may therefore include strontianite of thermophilic bacterial origin.

AUTHOR'S CONTRIBUTION

RM carried out the energy dispersive X-ray elemental analysis and powder X-ray diffraction analysis of mineralized thin film. KK participated in the elemental analysis of mineral crystals by ICP. NY participated in the design, coordination of the study and contributed in the drafting of the manuscript. All authors read and approved the final manuscript.

SOURCE OF FUNDING

The research was funded by Japan Science and Technology Agency Grant to feasibility study (FS) stage (AS251Z01973M).

TRANSPARENCY DECLARATION

The authors have no conflict of interest to declare.

REFERENCES

1. Finlay IG, Mason MD, Shelley M. Radioisotopes for the palliation of metastatic bone cancer: a systematic review. *Lancet Oncol.* 2005; 6: 392-400.
2. Simmons EC. Strontium: element and geochemistry. In: *Geochemistry*. Springer Netherlands. 1998: 598-599.
3. Yoshida N, Higashimura E, Saeki Y. Catalytic biomineralization of fluorescent calcite by the thermophilic bacterium *Geobacillus thermoglucosidasius*. *Appl Environ Microbiol.* 2010; 76: 7322-7327.
4. Murai R, Yoshida N. *Geobacillus thermoglucosidasius* endospores function as nuclei for the formation of single calcite crystals. *Appl Environ Microbiol.* 2013; 79: 3085-3090.
5. Hori M, Sano Y, Ishida A, Takahata N, Shirai, Watanabe T. Middle Holocene daily light cycle reconstructed from the strontium/calcium ratios of a fossil giant clam shell. *Scientific Reports.* 2015; 5: 8734.
6. Arai T, Chino N. Influence of water salinity on the strontium: calcium ratios in otoliths of the giant mottled eel, *Anguilla marmorata*. *Environ Biol Fishes.* 2017; 100: 281-286.
7. Lide DR. Physical constants of organic compounds. *CRC Handbook of chemistry and physics.* 2005; 89: 3-1.
8. Hepbasli A, Akdemir O. Energy and exergy analysis of a ground source (geothermal) heat pump system. *Energy Convers Manag.* 2004; 45: 737-753.
9. Self SJ, Reddy BV, Rosen MA. Geothermal heat pump systems: Status review and comparison with other heating options. *Appl Energy.* 2013; 101: 341-348.
10. Wellsbury P, Goodman K, Barth T, Cragg BA, Barnes SP, Parkes RJ. Deep marine biosphere fuelled by increasing organic matter availability during burial and heating. *Nature.* 1997; 388: 573-576.
11. Gold T. The deep, hot biosphere. *Natl Acad Sci USA.* 1992; 89: 6045-6049.
12. Gold T. The deep hot biosphere: the myth of fossil fuels. Springer Science & Business Media. 2013.
13. Kotelnikova S, Pedersen K. Evidence for methanogenic archaea and homoacetogenic bacteria in deep granitic rock aquifers. *FEMS Microbiol Rev.* 1997; 20: 339-349.
14. Igarashi K, Kato S. Extracellular electron transfer in acetogenic bacteria and its application for conversion of carbon dioxide into organic compounds. *Appl Microbiol Biotechnol.* 2017; 101: 6301-6307.
15. Sakai S, Nakashimada Y, Yoshimoto H, Watanabe S, Okada H, Nishio N. Ethanol production from H₂ and CO₂ by a newly isolated thermophilic bacterium, *Moorella* sp. HUC22-1. *Biotechnol Lett.* 2004; 26: 1607-1612.
16. Rabemanantsoa H, Kuninori Y, Saka S. High conversion efficiency of Japanese cedar hydrolyzates into acetic acid by co-culture of *Clostridium thermoaceticum* and *Clostridium thermocellum*. *J Chem Technol Biotechnol.* 2016; 91(4): 1040-1047.
17. Basen M, Müller V. "Hot" acetogenesis. *Extremophiles.* 2017; 21: 15-26.
18. Cozzarelli IM, Baedeker MJ, Eganhouse RP, Goerlitz DF. The geochemical evolution of low-molecular-weight organic acids derived from the degradation of petroleum contaminants in groundwater. *Geochim Cosmochim Acta.* 1994; 58: 863-877.
19. Murai R, Yoshida N. Magnesium-calcite crystal formation mediated by the thermophilic bacterium *Geobacillus thermoglucosidasius* requires calcium and endospores. *Curr Microbiol.* 2016; 73: 696-703.
20. Schultze-Lam S, Beveridge TJ. Nucleation of celestite and strontianite on a cyanobacterial S-layer. *Appl Environ Microbiol.* 1994; 60: 447-453.

Effects of cobalt and manganese on biomass and nitrogen fixation yields of a free-living nitrogen fixer - *Azotobacter chroococcum*

Justina Orji, Chima Ngumah*, Hanna Asor, Anulika Anuonyemere

Federal University of Technology Owerri, Department of Microbiology, P.M.B 1526 Owerri, Nigeria

*Corresponding author: Chima Ngumah; E-mail: ccngumah@yahoo.com

Received: 27 November 2017; **Revised submission:** 15 January 2018; **Accepted:** 22 January 2018

Copyright: © The Author(s) 2018. European Journal of Biological Research © T.M.Karpiński 2018. This is an open access article licensed under the terms of the Creative Commons Attribution Non-Commercial 4.0 International License, which permits unrestricted, non-commercial use, distribution and reproduction in any medium, provided the work is properly cited.

DOI: <http://dx.doi.org/10.5281/zenodo.1157098>

ABSTRACT

The effects of different concentrations of cobalt and manganese on the biomass and the ability of *Azotobacter chroococcum* to fix nitrogen were investigated. *In vitro* trials were conducted in Jensen's (nitrogen free) broth (half strength) under continuous air flow, incubated at ambient room temperatures for seven days. Results obtained showed that 12.5 mg/l, 25 mg/l, 50 mg/l, 100 mg/l, and 200 mg/l concentrations of cobalt and manganese respectively enhanced microbial growth of *Azotobacter chroococcum* concomitantly. However, nitrogen fixation was enhanced only at 12.5 mg/l and 25 mg/l concentrations for cobalt, and only at 12.5 mg/l concentration for manganese. Statistical analysis revealed no significant difference in the specific growth rates and nitrogen fixations respectively, between the cobalt and manganese trials. Kinetic modeling revealed that nitrogen fixation was associated with biomass concentration, and not with cell mass growth.

Keywords: Diazotroph; Micronutrients; Biostimulation; Toxicity; Luedeking-Piret model.

1. INTRODUCTION

Nitrogen is the most abundant element in the earth's atmosphere. However, due to the fact that atmospheric nitrogen is extremely un-reactive, it is also the most limiting nutrient to most plants [1]. Nitrogen is a constituent of proteins, enzymes, chlorophyll, and plant growth regulators; and its deficiency causes reduced growth and increased functional stress [2]. Biological nitrogen fixation is the process of converting elemental nitrogen into the forms, ammonium (NH_4^+) and nitrates (NO_3^-), available to plants [3], which are subsequently incorporated into amino acids [4]. Nitrogen fixation is the second most important biological process after photosynthesis, and it is mediated exclusively by prokaryotes [2]. Some bacteria fix nitrogen in a free living state (non-symbiotic fixation). Others are closely associated with plant roots (associative nitrogen fixation), and still others form a mutualistic symbiosis [4].

Although free living nitrogen fixing organisms are widely distributed in soils, the quantity of nitrogen they fix seldom approaches that of the symbiotic systems. It is not that they are inherently incapable of vigorous nitrogen fixation, but abundant substrates to support their growth and fixation are commonly lacking in the soil;

whereas, plants can directly supply the high energy demands of this process in associative and symbiotic systems [5]. The nitrogen fixing activity of non-symbiotic, non-photosynthetic aerobic bacteria is strongly dependent on favourable moisture conditions, oxygen concentrations, and a supply of organic carbon substrates [6]. Nitrogen fixers are generally more active in rhizosphere soil; with plants that are capable of releasing exudates promoting higher nitrogen fixation in soil [7].

Azotobacter species are free living, obligate aerobic nitrogen fixers dominantly found in soils. They are also capable of growth under low oxygen tension [8]. *Azotobacter species* are non-symbiotic heterotrophic bacteria capable of fixing an average of 20 kg N/ha/year. They also produce plant growth promoting substances and are known to be antagonistic to plant pathogens [2]. *Azotobacter chroococcum* is the most prevalent species found [9], but other species include *A. vinelandii*, *A. beijerinckii*, *A. armeniacus*, *A. nigricans*, and *A. paspali* [10].

Micronutrients are important components of biological systems; they are required at low concentrations for growth and metabolic functions. These essential elements serve several functions: they represent prosthetic groups in many proteins and dictate the configuration of the active sites of enzymes; they serve as co-factors for some enzymatic reactions; they serve as multidentate centres for porphyrin molecules; and they serve as redox centres, transferring electrons in important redox reactions in cells - these functions are not mutually exclusive [11]. Some essential micronutrients are Cu, Zn, Fe, Ni, Mn, and Co. Microbes have evolved mechanisms that vary in specificity to accumulate these micronutrients from the surrounding environment [12].

The objectives of this study were to: determine the nitrogen fixing capacity of *Azotobacter chroococcum* in pure culture; measure the effects of different concentrations of cobalt and manganese (as CoCl_2 and MnCl_2) respectively on the nitrogen fixing capacity and cell mass growth of *A. chroococcum*; to explore the relationship between the nitrogen fixing capacity of *A. chroococcum* and its cell mass growth at different concentrations of cobalt and manganese respectively.

2. MATERIALS AND METHODS

2.1. Collection of soil samples

Rhizosphere soil samples were collected from *Musa paradisiaca* (plantain). Soil samples were collected at a depth of about 10-20 cm using sterile corers (sterilized with 95% ethanol). Soil samples were then passed through a coarse sieve (< 2 mm) to pulverize, remove any foreign material, and thoroughly mix them. Soil samples were transported to the laboratory in sterile containers at 4°C, where they were kept refrigerated at 4°C until required for analysis.

2.2. Isolation of test isolate (*Azotobacter chroococcum*)

10 g soil sample was homogenized in 90 ml sterile distilled water (with agitation for 15 minutes), and serially diluted in sterile distilled water in a proportion of 1:10 up to 10^9 . 0.1 ml aliquot from each dilution was inoculated onto sterile solid Jensen's (nitrogen free) agar plates, and plated out using the spread plate method. Plates were incubated at prevailing room temperatures for 3-7 days. Discrete colonies were enumerated, and sub-cultured severally on Jensen's agar (SRL, India) to get axenic cultures. Pure isolates were stored on Jensen's agar slants at 4°C.

2.3. Microbial analysis

The colonial morphology of pure isolates on agar plates were observed and recorded. Isolates were Gram-stained, spore-stained, and subjected to different biochemical tests: motility test; oxygen utilization test; catalase test; utilization of rhamnose, caproate, caprylate, meso-inositol, mannitol, malonate. Bacteria isolates were identified by comparing their morphological, microscopic, and biochemical characteristics with those of known taxa using the schemes of Bergey's Manual of Determinative Bacteriology [10].

2.4. Determination of effects of cobalt and manganese concentrations on the cell growth and nitrogen fixing capacity of *Azotobacter chroococcum*

A stock broth culture of *A. chroococcum* was prepared. To prepare stock broth culture of *A. chroococcum*, a sterile wire loop was used to introduce *A. chroococcum* from Jensen's agar slant to sterile Jensen's (nitrogen free) broth (Jensen's medium manufactured by Sisco Research Laboratory PVT. Ltd, Mumbai, India), and incubated at prevailing room temperatures for 7 days under continuous airflow. From this stock broth, 0.5 McFarland standards were prepared [2]. Then 200 mg/l, 100 mg/l, 50 mg/l, 25 mg/l, 12.5 mg/l, and 0 mg/l sterile CoCl_2 and MnCl_2 solutions were prepared in half strength Jensen's broth [11]. Then 0.1 ml aliquot of 0.5 McFarland standard of *A. chroococcum* was added to 9.9 ml of each of the above sterile CoCl_2 and MnCl_2 solutions (concentration). This set up was incubated for 7 days at prevailing room temperatures under continuous airflow in a sterile chamber plugged to a Airfree T800 Filterless Air Purifier, (USA). The optical density at 600nm (OD_{600}) (using model 722 visible spectrophotometer, manufactured by Shanghai Third instrument Factory, China), nitrate-N concentration, and amino-N concentration of each test was measured at days 0 and 7 respectively [13].

2.5. Determination of nitrate nitrogen and amino nitrogen

Broth culture experiments were analyzed for nitrate nitrogen ($\text{NO}_3\text{-N}$) and amino nitrogen (Amino-N) at inception (Day 0) and at the end (Day 7) of the experiment. Nitrate-N concentration was determined by Cataldo's method [14]: 2.5 μl of sample solution was taken into a 1.5 ml Eppendorf tube, and 10 μl of salicylic acid-sulfate solution (500 mg of salicylic acid was dissolved in 10 ml of concentrated sulfuric acid) was mixed and kept for 20 minutes. Then, 250 μl of 2M NaOH solution (8.00 g of NaOH was dissolved in 100 ml of water) was mixed and kept for 20 minutes. 200 μl of the reaction solution was put in a 722 visible spectrophotometer and the absorption at 410 nm was measured. Standard solution was made by dissolving

42.5 mg of NaNO_3 in 100 ml of water, which contains 5 mM nitrate (70 mg N l^{-1}). Diluted solutions (0, 1, 2, 3, 4, 5 mM) were used for the calibration and plotting of standard curve.

Amino-N concentration was determined by ninhydrin method [15]: 2.5 μl of sample solution was taken into a 1.5 ml Eppendorf tube, and 75 μl of citrate buffer (5.6 g of citrate and 2.13 g of NaOH was dissolved in 100 ml of water) was mixed. Afterwards, 60 μl of ninhydrin solution (958 mg of ninhydrin and 33.4 mg of ascorbate was dissolved in 3.2 ml of water and filled up to 100 ml with methoxyethanol in a flask. The flask was secured with its cork and heated at 100°C for 20 minutes in a hot air oven (Quincy Hydraulic Gravity Convection Oven, USA.). Then, 300 μl ethanol was added and cooled to room temperature for 10 minutes. 200 μl of the reaction solution was put in a 722 visible spectrophotometer and the absorption at 570 nm was measured. Standard solution was made by dissolving 66.1 mg of asparagine (or 70.1 mg of asparagine monohydrate) plus 73.1 mg glutamine in 100 ml of water, which contains 5 mM asparagine + 5 mM glutamine (280 mg N L^{-1}). Diluted solutions (0, 28, 56, 84, 112, 140 mg N L^{-1}) were used for the calibration and plotting of standard curve.

2.6. Determination of specific growth rate

The specific growth rate of *Azotobacter chroococcum* was determined using the formula proposed by Stanier et al. [16].

$$\text{Specific growth rate} = \frac{\text{Log OD}_1 - \text{Log OD}_0}{T_1 - T_0} \times 2.303$$

Where,

Log OD_1 = Log value of optical density (OD) of culture at time T_1 days

Log OD_0 = Log value of optical density (OD) of culture at time T_0 days.

2.7. Estimation of nitrogen fixed

The amount of nitrogen fixed was estimated with the formula:

$$\text{Nitrogen fixed} = N - N_0$$

Where,

N = the total concentrations of nitrate nitrogen and amino nitrogen in culture medium after incubation

N_0 = the total concentrations of nitrate nitrogen and

amino nitrogen in culture medium before incubation (at inception).

2.8. Estimation of nitrogen fixation rate

Nitrogen fixation rate was estimated using the formula:

$$\text{Nitrogen fixation rate} = \frac{N - N_0}{T - T_0}$$

Where,

$N - N_0$ = Nitrogen fixed

$T - T_0$ = incubation period

2.9. Statistical analysis

All measurements were made in triplicate, and values reported as mean of triplicate values. Student t tests and Pearson's correlation analysis for all possible variable pairs were estimated using Minitab 17 software. Significant difference was taken at 5% level of significance ($p < 0.05$).

2.10. Kinetic modeling for product synthesis (nitrogen fixation)

The Luedeking-Piret model was applied to analyze product synthesis (nitrogen fixation) kinetics, using Curve Expert Professional 2.4.

3. RESULTS AND DISCUSSION

Experimental data revealed that the trials with no micronutrient (Co and Mn) added (control)

had a cell mass yield of $X_0 = 0.042 \text{ OD}_{600}$ units, and a nitrogen fixation yield of $P_0 = 0.847 \text{ ppm}$ respectively, after seven days incubation. Similarly, experimental data revealed maximum cell mass concentrations, X_{max} , (which occurred at 200 mg/l for both cobalt and manganese) of 0.100 OD_{600} units and 0.092 OD_{600} units for cobalt and manganese respectively (plots not shown).

Cobalt enhanced nitrogen fixation of *Azotobacter chroococcum* at 12.5 mg/l and 25 mg/l CoCl_2 concentrations, while 50 mg/l, 100 mg/l, and 200 mg/l CoCl_2 concentrations abated the nitrogen fixation of *A. chroococcum*. On the other hand, manganese enhanced nitrogen fixation of *Azotobacter chroococcum* at 12.5 mg/l MnCl_2 concentration, while 25 mg/l, 50 mg/l, 100 mg/l, and 200 mg/l MnCl_2 concentrations abated the nitrogen fixation of *A. chroococcum* (Figure 1). Figure 1 also showed that maximum nitrogen fixations, P_{max} , occurred at 12.5 mg/l concentration for both cobalt (1.936 ppm) and manganese (1.368 ppm) respectively.

Contrary to the results of nitrogen fixation, the specific growth rate of *A. chroococcum* was enhanced by all the micronutrient concentrations tested for both cobalt and manganese; with specific growth rate increasing concurrently with increasing cobalt and manganese concentrations respectively. Thus, in these experiments, increase in cell mass of *A. chroococcum* did not always translate to increase in nitrogen fixation. Maximum growth rates, μ_{max} , recorded for Co and Mn were 0.131 OD units/day and 0.119 OD units/day respectively.

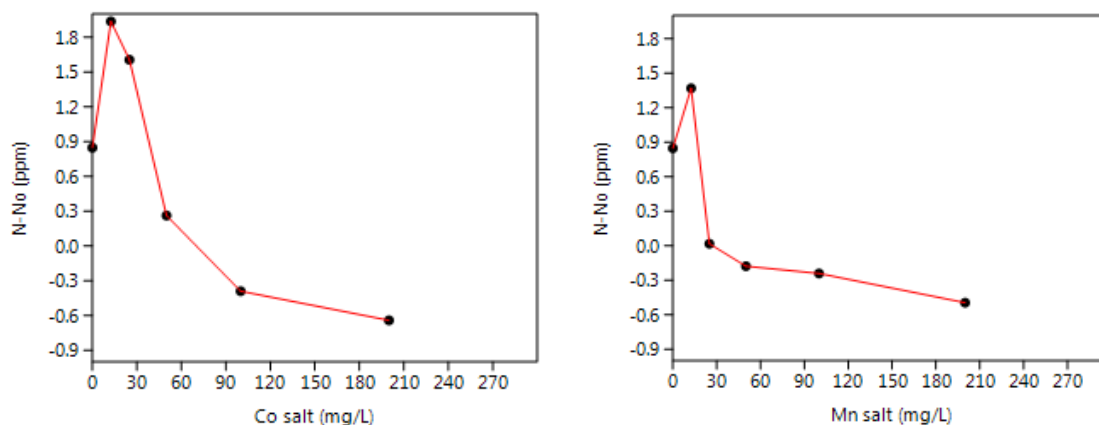


Figure 1. Nitrogen fixation yields of *Azotobacter chroococcum* at different cobalt and manganese concentrations.

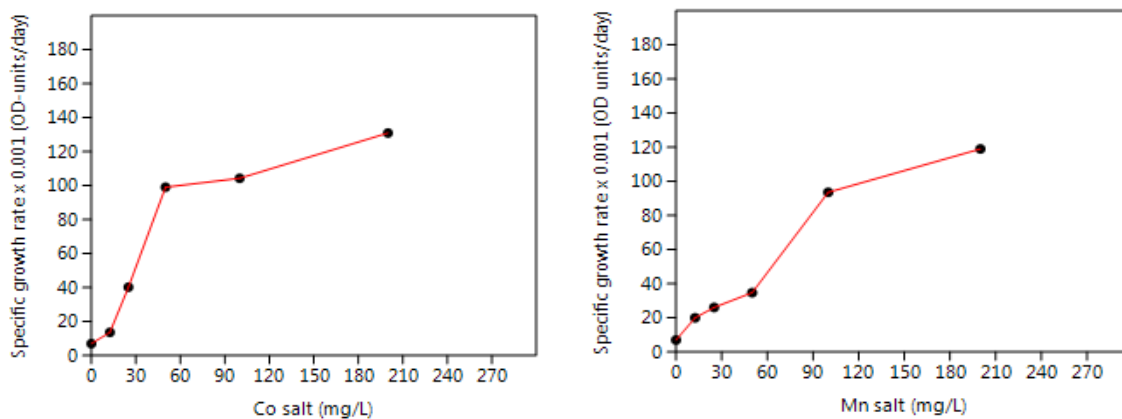


Figure 2. Specific growth rates of *Azotobacter chroococcum* at different cobalt and manganese concentrations.

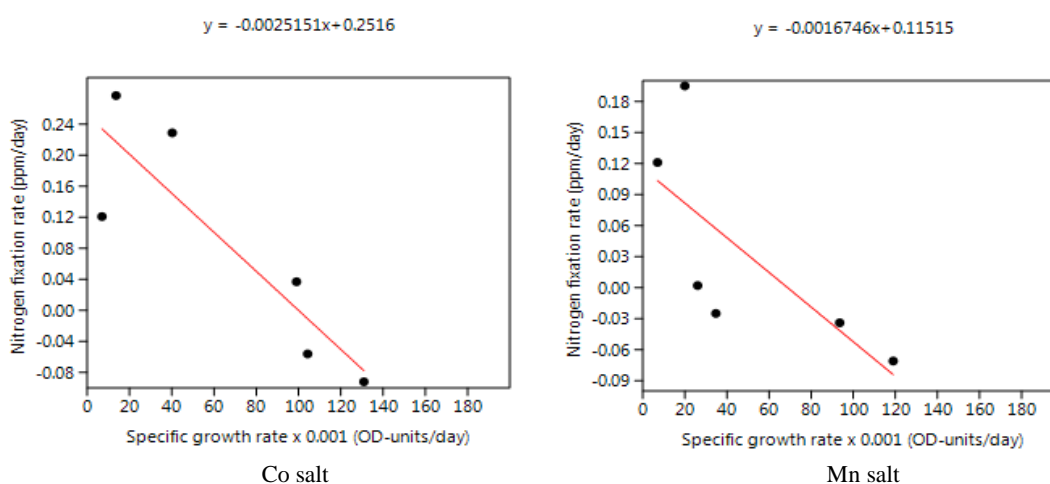


Figure 3. Luedeking-Piret model of *Azotobacter chroococcum* for different of cobalt and manganese concentrations.

Though experiments revealed comparatively higher nitrogen fixation and specific growth rate values in cobalt trials, Student t tests showed no significant difference ($p > 0.05$) in the specific growth rates and nitrogen fixation rates respectively between the cobalt and manganese broth trials of *A. chroococcum*. Pearson’s correlation analysis showed very strong and direct correlations ($p < 0.05$) between micro-element (Co and Mn) concentrations and cell mass growth, with coefficient of correlations (r) of 0.913 and 0.975 for Co and Mn respectively. However, correlations between micro-element concentrations and amount of nitrogen fixed were indirect and relatively weaker, with coefficient of correlations (r) of -0.822 ($p < 0.05$) and -0.732 ($p > 0.05$) for Co and Mn respectively. This indirect relationship between nitrogen fixation and population size was also reported by Chang and Knowles [17].

The Leudeking-Piret model [18] was applied to determine the type of relationship existing between cell mass and nitrogen fixation by *A. chroococcum in vitro*.

$$r_{fp} = \alpha r_{fx} + \beta x \tag{1}$$

Where,

r_{fp} = rate of product formation

r_{fx} = rate of biomass formation

α = coefficient of proportionality between the rate of product formation and growth rate (ppm/OD-units)

β = coefficient of proportionality between the rate of product formation and biomass concentration (ppm/OD-units/day).

According to this model, the product formation rate (nitrogen fixation rate) depends linearly upon the growth rate and the cell mass concentration.

$$\frac{\delta P}{\delta t} = \alpha \frac{\delta x}{\delta t} + \beta x \tag{2}$$

$$\beta = \frac{(dP/dt) \text{ stationary phase}}{X_s} \quad (3)$$

X_s = cell concentration at stationary phase

The other kinetic constant, α , can be calculated using the yield coefficient, $Y_{p/x}$, which is given as:

$$Y_{p/x} = \frac{\text{Mass of product formed}}{\text{Mass of cell formed}} = \frac{\Delta P}{\Delta X} = \frac{P - P_0}{X - X_0} \quad (4)$$

Integrating equation 3 gives:

$$P(t) - P(0) - \beta(X_s/k) [1 - X_0/X_s (1 - e^{-kt})] = \alpha(X_t - X_0) \quad (5)$$

A linear plot of nitrogen fixation rate against specific growth rate generated α and β coefficients for Co and Mn respectively (Figure 3). For Co, $\alpha = -0.0025151$ and $\beta = 0.2516$; while for Mn, $\alpha = -0.0016746$ and $\beta = 0.11515$. If $\alpha \leq 0$, then nitrogen fixation is associated with cell mass concentration; on the other hand, if $\beta \leq 0$, then nitrogen fixation is associated with cell mass growth; however, if $\alpha > 0$ and $\beta > 0$, then nitrogen fixation is associated with both cell mass growth and cell mass concentration [19]. From the results obtained in this work, nitrogen fixation (product synthesis rate) of *A. chroococcum* was associated with cell mass concentration, X_c , and not with cell (bacterial) mass growth (for both Co and Mn trials). According to Wright and Weaver [20], a sizeable population may be present without providing the enzyme activity needed for significant rates of nitrogen fixation; nevertheless at the attainment of a critical population size the needed biomass and nitrogenase for significant rates of nitrogen fixation is provided. Since nitrogen fixation in both experiments depend solely on biomass concentration, it implies that the substrates consumed (Co and Mn) were required for both the fixation of nitrogen and also for the growth of *A. chroococcum* [21]. Also since nitrogen fixation was solely dependent on biomass concentration for Co and Mn, it means that the nitrogen fixed by *A. chroococcum* in these trials is a secondary metabolite [22]. When non-growth associated product formation is modeled as a phenomenon associated with the secondary metabolite formation, the rate of the product formation is linked to the endogenous rate of the cellular degradation (endogenous metabolism). The product formation is thus a process that is secondary to the biomass growth. In addition, Zerajic and Savkovic-Stevanovic [23] stated that in such a situation, product formation but not growth is subsequently

inhibited by the concentration of the substrate. This phenomenon expressed by Stevanovic [23] agrees with the data obtained in this work, where after a certain concentration, increased Co and Mn concentrations concurrently abated nitrogen fixation, but still enhanced cell mass growth.

4. CONCLUSIONS

The results obtained in this study suggest that the micronutrients, cobalt and manganese, impacted both on the cell mass growth and nitrogen fixation of *Azotobacter chroococcum*, but in different ways. All the concentrations of cobalt and manganese tested enhanced cell mass growth, while at given concentrations nitrogen fixation started to wane for both cobalt and manganese. Nitrogen fixation was found to be associated with biomass density, rather than with cell mass growth.

Further studies are recommended were similar investigations may be done *in situ* in soil, and compared with *in vitro* results.

AUTHOR'S CONTRIBUTION

JO: Project supervisor, research design; CN: Research design/development, experimental design, mathematical/statistical analysis; HA: Sample collection and laboratory assistance; AA: Sample collection and laboratory assistance. All authors read and approved the final manuscript.

TRANSPARENCY DECLARATION

The authors have no conflict of interest to declare.

REFERENCES

1. Shridhar BS. Review: nitrogen fixing microorganisms. *Int J Microbiol Res.* 2012; 3(1): 46-52.
2. Kizilkaya R. Nitrogen fixation capacity of *Azotobacter* spp. strains isolated from soils in different ecosystems and relationship between them and the microbiological properties of soils. *J Environ Biol.* 2009; 30(1): 73-82.
3. Simon Z, Mtei K, Gessesse A, Ndakidemi PA. Isolation and characterization of nitrogen fixing rhizobia from cultivated and uncultivated soils of northern Tanzania. *Am J Plant Sci.* 2014; 5: 4050-4067.
4. Myrold DD. Quantification of nitrogen transformations. In: Hurst CJ, Crawford RL, Knudsen

- GR, Mcinerney MJ, Stetzenbach LD, eds. Manual of environmental microbiology. ASM Press, 2002: 583-590.
5. Burris RH. Nitrogen fixation. In: eLS. John Wiley & Sons Ltd. 2004. DOI: 10.1038/npg.els.0000626.
 6. Matthew CJ, Bjorkman MK, David MK, Saito AM, Zehr PJ. Regional distributions of nitrogen-fixing bacteria in the Pacific Ocean. *Limnol Oceanogr.* 2008; 53: 63-77.
 7. Egamberdieva D, Kucharova Z. Cropping effects on microbial population and nitrogenase activity in saline arid soil. *Turk J Biol.* 2008; 32: 85-90.
 8. Gonzalez LJ, Rodelas B, Pozo C, Salmeron V, Martinez MV, Salmeron V. Liberation of amino acids by heterotrophic nitrogen fixing bacteria. *Amino Acids.* 2005; 28: 363-367.
 9. FAO: Application of nitrogen fixing systems in soil improvement and management. Food and Agriculture Organization of the United Nations. FAO Soils Bulletin 49, Rome 1982.
 10. Holt JG, Kreig NR, Sneath PH, Staley JT, Williams ST, eds. *Bergey's Manual of Determinative Bacteriology*, 9th edn. Williams & Wilkins, 1994.
 11. Mills AL. Metal requirements and tolerance. In: Hurst CJ, Crawford RL, Knudsen GR, Mcinerney MJ, Stetzenbach LD, eds. *Manual of Environmental Microbiology*. ASM Press, 2002: 456-465.
 12. Gadd GM. Heavy metal accumulation by bacteria and other microorganisms. *Experientia.* 1990; 46(8): 834-840.
 13. Paudyal SP, Aryal RR, Chauhan SV, Maheshwari DK. Effect of heavy metals on growth of *Rhizobium* strains and symbiotic efficiency of two species of tropical legumes. *Scientific World.* 2007; 5(5): 27-32.
 14. Cataldo KA, Schrader LE, Youngs VL. Analysis by digestion and colorimetric assay of total nitrogen in plant tissues high in nitrate. *Crop Sci.* 1974; 14: 845-846.
 15. Herridge DF. Effect of nitrate and plant development on the abundance of nitrogen solutes in root-bleeding and vacuum-extracted exudates of soybean. *Crop Sci.* 1984; 24: 173-179.
 16. Stanier RY, Adelberg EA, Ingraham JL. Microbial growth. In: *General Microbiology*. MacMillan Publication, London, 1985: 273-293.
 17. Chang PC, Knowles R. Non-symbiotic nitrogen fixation in some Quebec soils. *Can J Microbiol.* 1965; 11: 29-38.
 18. Luedeking R, Piret EL. A kinetic study of the lactic acid fermentation. Batch process at controlled pH. *J Biochem Microbiol Technol Engin.* 1959; 1(4): 393-412.
 19. Ramakrishnan V, Goveas LC, Halami PM, Narayan B. Kinetic modeling production and characterization of an acidic lipase produced by *Enterococcus durans* NCIM5427 from fish waste. *J Food Sci Technol.* 2015; 52(3): 1328-1338.
 20. Wright SF, Weaver RW. Enumeration and identification of nitrogen fixing bacteria from forage grass roots. *Appl Env Microbiol.* 1981; 42(1): 97-101.
 21. Ahmad F, Jameel AT, Kamarudin MH, Mel M. Study of growth kinetics and modeling of ethanol production by *Saccharomyces cerevisiae*. *Afr J Biotechnol.* 2011; 16(81): 18842-18846.
 22. Vazquez JA, Murado AM. Unstructured mathematical model for biomass lactic acid and bacteriocin productions by lactic acid bacteria in batch fermentation. *J Chem Technol Biotechnol.* 2008; 83(1): 91.
 23. Zerajic S, Savkovic-Stevanovic J. The kinetic models of the bioprocess with free and immobilized cells. *CI & CEQ.* 2007; 13(4): 216-226.

Neurospora tetraspora D. Garcia, Stchigel & Guarro (= *Gelasinospora tetrasperma* Dowding) as a first record to Egypt

A. H. Moubasher^{1,2*}, M. A. Abdel-Sater^{1,2}, Zeinab Soliman²

¹ Department of Botany and Microbiology, Faculty of Science, Assiut University, P.O. Box 71526, Assiut, Egypt

² Assiut University Mycological Centre, Assiut University, P.O. Box 71526, Assiut, Egypt

*Corresponding author: A. H. Moubasher; E-mail: ahamaumc@yahoo.com

Received: 09 December 2017; Revised submission: 30 January 2018; Accepted: 05 February 2018

Copyright: © The Author(s) 2018. European Journal of Biological Research © T.M.Karpiński 2018. This is an open access article licensed under the terms of the Creative Commons Attribution Non-Commercial 4.0 International License, which permits unrestricted, non-commercial use, distribution and reproduction in any medium, provided the work is properly cited.

DOI: <http://dx.doi.org/10.5281/zenodo.1165603>

ABSTRACT

An interesting isolate of homothallic, ascosporic filamentous fungus having 4-spored asci, was recovered once from a non-rhizosphere soil sample collected from a grapevine plantation in the village of El-Khawaled, Sahel-Saleem city, Assiut. It was isolated on DYM agar plate at 25°C in June 2008. The isolate was identified phenotypically and genotypically as *Neurospora tetraspora* (= *Gelasinospora tetrasperma*) and was deposited in the culture collection of Assiut University Mycological Centre as AUMC no. 6784 and ITS gene sequence of the strain was deposited at the National Center for Biotechnology Information (NCBI) and assigned a GenBank accession number JQ425383. *N. tetraspora* is being recorded in the current work for the first time in Egypt. By this addition, the genus is now known in Egypt by four species. A key is provided for the four species.

Keywords: Assiut; Grapevine; Genotypic and phenotypic characterization; ITS; Soil.

1. INTRODUCTION

During the course of a survey of mycobiota of grapevine plantations in Assiut Governorate, Egypt in 2008/2009, an interesting ascosporic species was isolated from the soil by dilution-plate method [1] on dichloran yeast extract malt extract agar plate, DYM [2]. The macro- and micro-morphological characteristics of the isolate proved to be sufficiently similar to those of the genera *Neurospora*/*Gelasinospora* [3-6].

The generic name *Neurospora* was introduced by Shear & Dodge [3] for four species characterized by dark ascospores, with a grooved surface with longitudinal ribs. Later, numerous species were added [7-14] and so far 12 species have been accepted. In 1933, the genus *Gelasinospora* was erected by Dowding [15] to accommodate two species with ascospores similar to those of *Neurospora*, but with a pitted wall. Further species were added by others [4, 16-25].

The phylogenetic relationships between members of *Gelasinospora* and *Neurospora* were investigated by Dettman et al. [26] analysing four genes: ITS/5.8S rRNA, glyceraldehyde 3-phosphate dehydrogenase (*gpd*), mating-type *A-1*, and mating-type *a-1*. Although only five species of *Gelasino-*

spora were included in that study, they concluded that pitted vs. ribbed ascospores is not a useful criterion for the separation of these genera. Also, partial sequences of the 28S rDNA gene from 27 species of both genera were analysed by Garcia et al. [6] to infer their phylogenetic relationships. Species of the two genera were interspersed in the different clades and confirmed that they are genetically very similar. The name *Neurospora* has priority under the Code, and *Gelasinospora* was treated as a synonym of *Neurospora*, whose generic diagnosis is amended, and a dichotomous key to 49 species of *Neurospora* recognized in the genus was presented [6].

The internal transcribed spacer (ITS) region, located between the 18S and 28S rRNA genes, is an area of particular importance in discriminating between closely related species or at intraspecific level, because it has areas both of high conservation and high variability. ITS sequencing has been used to identify *Neurospora* species [6, 27].

In Egypt, of this genus only the anamorphic stage of *Neurospora crassa* (*Chrysonilia crassa*), the 4-spored ascospore species (*Neurospora tetrasperma*) and the 8-spored ascospore species *Neurospora hippopotama* (= *Gelasinospora hippopotama*) were reported. *N. crassa* has been reported from animal and bird pens materials [28], soybean meal [29], combine harvester sorghum dust [30], caraway and cumin seeds [31], the air of Bahariya Oasis, Western Desert [32], grapevine soil, Assiut [33]. *N. hippopotama* (J.C. Krug, R.S. Khan & Jeng) D. Garcia, Stchigel & Guarro (= *Gelasinospora hippopotama* Krug, Khan & Jeng) was first isolated and described from sandy soil, Dakhleh Oasis, Western Desert in 1994 [24]. Also, *N. tetrasperma* was recently recorded from the air of citrus plantations in Sahel-Saleem city, Assiut, Egypt [34].

2. MATERIALS AND METHODS

2.1. Strain examined

The strain examined was isolated from a soil sample collected from a grapevine plantation in El-Khawaled village, Sahel-Saleem city at approximately 25 km south-east of Assiut town, Egypt (about 6 km to the east border of the river Nile). The strain was isolated in June 2008, on

dichloran yeast extract malt extract agar, DYM [2] at 25°C, by Zeinab Soliman in a laboratory of Assiut University Mycological Centre (AUMC), Assiut, Egypt. It was misidentified as *Gelasinospora bonaerensis* [33] based on its ITS sequence similarity with the type strain (99%). However, the strain produces 4-spored asci and that of *G. bonaerensis* 8-spored asci.

2.2. Morphology

For macromorphological observations, the strain was grown in the dark on Czapek yeast autolysate agar (CYA) and potato sucrose agar (PSA) at 25°C for 7 days (for medium formulations see Samson et al. [35]). For micromorphological observations, microscopic mounts were made in lactophenol cotton blue from PSA plates after 10-15 day-old culture.

2.3. Growth of the fungus and DNA extraction and sequencing

The fungus was grown on CYA plates and incubated at 25°C for 7 days. A small amount of fungal mycelia was scraped and suspended in 100 µl of distilled water and boiled at 100°C for 15 minutes and stored at -70°C. Samples were sent to SolGent Company (Daejeon, South Korea) to carry out the whole procedure from DNA extraction till the final step of DNA sequencing. Fungal DNA was extracted and isolated using SolGent purification bead. Internal transcribed spacer (ITS) sequences of nuclear ribosomal DNA were amplified using universal primers: ITS 1 (5' - TCC GTA GGT GAA CCT GCG G - 3'), and ITS 4 (5' - TCC TCC GCT TAT TGA TAT GC - 3'). Then amplification was performed using the polymerase chain reaction (PCR) (ABI, 9700). The PCR reaction mixtures were prepared using Solgent EF-Taq as follows: 10X EF-Taq buffer 2.5 µl, 10 mM dNTP (T) 0.5 µl, primer (F-10p) 1.0 µl, primer (R-10p) 1.0 µl, EF-Taq (2.5U) 0.25 µl, template 1.0 µl, DW to 25 µl. Then the amplification was carried out using the following PCR reaction conditions: one round of amplification was performed consisting of denaturation at 95°C for 15 min followed by 30 cycles of denaturation at 95°C for 20 sec, annealing at 50°C for 40 sec and extension at 72°C for 1 min,

with a final extension step of 72°C for 5 min.

Then the PCR products were purified with the SolGent PCR Purification Kit-Ultra (SolGent, Daejeon, South Korea) prior to sequencing. Then the purified PCR products were reconfirmed (using size marker) by electrophoreses of the PCR products on 1% agarose gel. Then these bands were eluted and sequenced. Each sample was sequenced in the sense and antisense direction. Contigs were created from the sequence data using the CLCBio Main Workbench program. The sequence obtained was further analyzed using BLAST from the National Center of Biotechnology Information (NCBI) website. Sequence obtained together with those retrieved from the GenBank database (<http://www.ncbi.nlm.nih.gov>) were subjected to the Clustal W analysis using MegAlign software version 5.05 (DNASTAR Inc., Madison, Wisconsin, USA) for the phylogenetic analysis [36].

3. RESULTS AND DISCUSSION

Neurospora tetraspora D. Garcia, Stchigel & Guarro 2004 = *Gelasinospora tetrasperma* Dowding, Can J Res 1933; 9(3): 294 = *Gelasinospora calospora* f. *tetrasperma* (Dowding) C. Moreau & M. Moreau 1951

3.1. Culture morphology

AUMC strain 6784 on PSA and CYA at 25°C after 7 days: colonies filling the agar plates (9 cm diam.), producing a rapid and dense growth of mycelium which is white at first, becoming gray or slightly pinkish (Fig. 1).

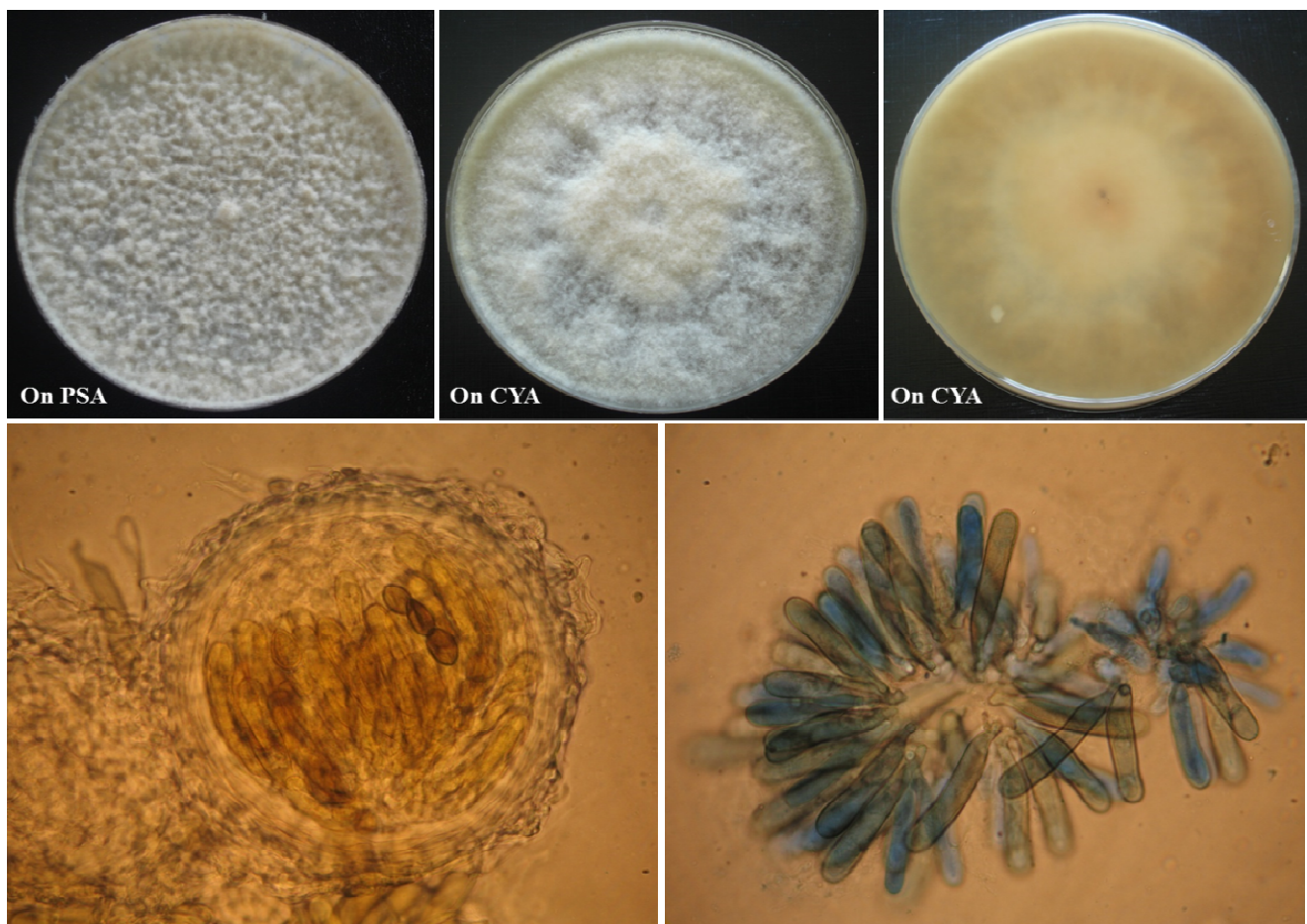


Figure 1. *Neurospora tetraspora* (*Gelasinospora tetrasperma*) AUMC 6784, 7-day-old colony obverse on PSA (upper left) and on CYA (upper middle) and reverse on CYA (upper right), ascoma (lower left) and asci (lower right).

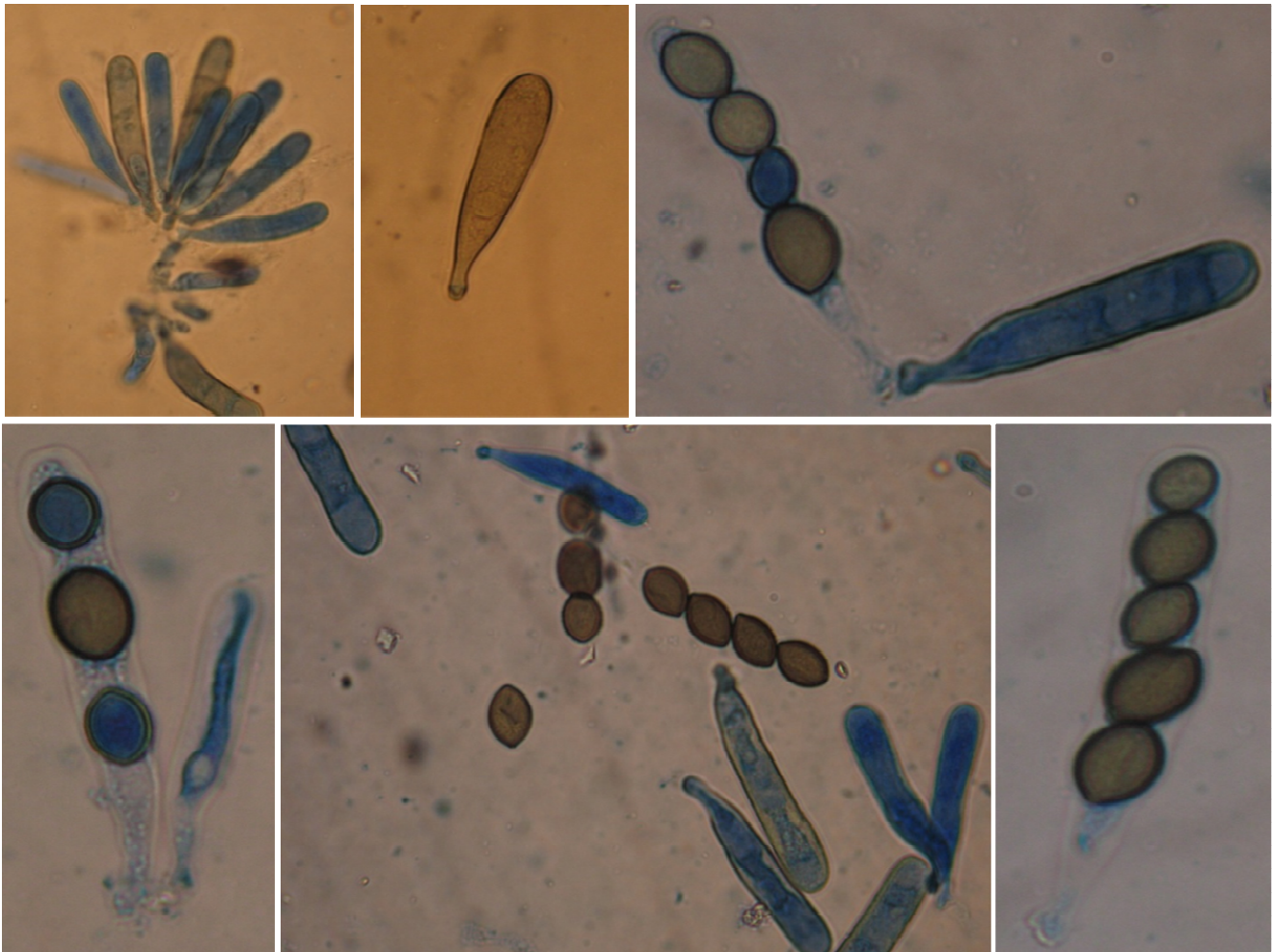


Figure 2. *Gelasinospora tetrasperma* AUMC 6784: asci and ascospores.

3.2. Micromorphology

Ascomata superficial or slightly immersed, black, pyriform, ostiolate, 450-600 x 270-450 μm . Asci cylindrical, 4-spored, but 3- and 5-spored asci were seen in the AUMC strain. Ascospores uniseriate, ellipsoidal or elongate, 22-33 x 12-20 μm , broadly rounded at the ends, dark brown, becoming black and opaque, walls with slightly irregular pits, one germ pore at each end (Figs. 1 & 2). Asexual stage (conidial state) not observed.

3.3. Genotypic characterization

Comparison of ITS sequence of AUMC strain 6784 with eight *Neurospora/Gelasinospora* species showed close similarity ranging from 97.91%-98.44%, with the highest ITS similarity to the type strains of *G. tetrasperma* (98.44%, with no gaps) and *G. udagawae* (98.44%, with 2 gaps) followed

by *N. dictyophora* (98.43%, with 1 gap) and *N. pannonica* (98.38%, with 2 gaps). The previous species along with those presented in Table 1 produce 8-spored asci, but only *G. tetrasperma* has 4-spored asci. Thus, morphological characteristics along with the highest ITS sequences similarity and no gaps with the type species confirmed its identity as *G. tetrasperma* (= *Neurospora tetraspora*) (Table 1, Fig. 3). From this finding, both molecular and phenotypic features are helpful in such identification.

3.4. Distribution

N. tetraspora (= *G. tetrasperma*) was found on dung of ptarmigan, horse, rabbit and cow from Ontario, Quebec, Manitoba, Venezuela, England and Germany and was also found on seeds of *Beta vulgaris* L. and *Festuca rubra* L. from Quebec [4] and from *Vaccinium* sp. in Quebec [37]. It was

also reported in Canada, England, Finland, Norway, Russia, Spain, Sweden, and USA, from dung and soil [6]. Also, *N. tetraspora* was one of the most frequent isolated ascomycete microfungi from rotting wood in Northern Alberta forests, Canada suggesting that these fungi are significant component of wood decaying fungal communities [38].

In the current study, it was reported from a non-rhizosphere soil sample collected from a grapevine plantation in El-Khawaled village, Assiut, Egypt. The presence of this fungus together with

other fungal communities in grapevine soil [33] may help in decaying the woody and non-woody debris of vine.

Living culture of the fungus is deposited at the culture collection of the Assiut University Mycological Centre (AUMC 6784), Assiut, Egypt. The strain is registered with a GenBank accession number JQ425383 (<http://www.ncbi.nlm.nih.gov>). It is worthy to mention that only 2 strains registered in the GenBank and these are CBS178.33^T=NR_077163 [27], GEN002=GQ922543 [39], in addition to ours.

3.5. Key to the four species of *Neurospora* so far recorded in Egypt

1. Homothallic 2
1. Heterothallic, asci 8-spored; ascospores with longitudinal striations, 27-36 x 14-16 µm; anamorph present, colonies orange, conidia 6-8 µm diam *N. crassa*
2. Asci 8-spored, ascospores pitted, 35-45 x 25-32 µm *N. hippopotama* (= *G. hippopotama*)
2. Asci 4-spored 3
3. Ascospores with longitudinal striations, (24-)31-36(-40) x 15-19(-22) µm, anamorph present *N. tetrasperma*
3. Ascospores pitted, 22-33 x 12-20 µm; anamorph absent *N. tetraspora* (= *G. tetrasperma*)

Table 1. The Assiut University Mycological Centre accession number, AUMC 6784 of *N. tetraspora* isolated from grapevine soil with its accession GenBank number together with the closest match in the GenBank database and sequence similarity in percent to the match as inferred from Blastn searches of ITS sequences.

AUMC number	Accession GenBank number	Length (bp)	Closest GenBank match # ITS	Sequencing similarity (%)	Gaps	Species	References
			CBS178.33 ^T =NR_077163	569/578 (98.44%)	0/578 (0%)	<i>G.tetrasperma</i>	[27]
			CBS 298.63 ^T =AY681176	575/587 (97.96%)	1/587 (0%)	<i>N. terricola</i>	[27]
			FGSC1889 ^T = NR_077131	544/554 (98.19%)	1/554 (0%)	<i>N. terricola</i>	[26]
			CBS 435.74 ^T =AY681184	569/579 (98.27%)	1/579 (0%)	<i>G. saitoi</i>	[27]
			CBS309.91 ^T =NR_103582	567/576 (98.44%)	2/576 (0%)	<i>G. udagawae</i>	[27]
6784	JQ425383	590	CBS 529.95 ^T =AY681181	565/574 (98.43%)	1/574 (0%)	<i>N. dictyophora</i>	[27]
			CBS 571.69 ^T =GQ922531	562/572 (98.25%)	2/572 (0%)	<i>N. africana</i>	[39]
			FGSC 1740 ^T =NR_077130	550/560 (98.21%)	2/560 (0%)	<i>N. africana</i>	[26]
			CBS561.94 ^T =NR_137146	562/574 (97.91%)	1/574 (0%)	<i>G. hippopotama</i>	[27]
			CBS 270.91 ^T =GQ922532	548/557 (98.38%)	2/557 (0%)	<i>N. pannonica</i>	[39]
			CBS315.74 ^T =NR_144834	508/596 (85.23%)	31/596 (5%)	<i>C. madrasense</i>	[40]

N = *Neurospora*, *G* = *Gelasinospora*, *C* = *Chaetomium*.

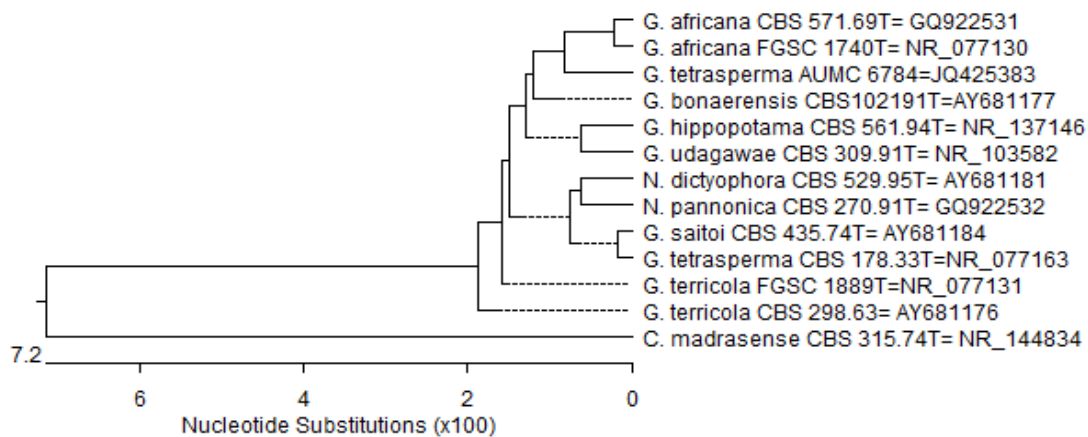


Figure 3. Phylogenetic tree based on DNA sequence data of ITS region of *N. tetrasperma* AUMC 6784 (= *G. tetrasperma*), compared with 11 reference strains in Genbank of closely related *Neurospora*/*Gelasinospora* species and *Chaetomium madrasense* as an outgroup.

ACKNOWLEDGEMENTS

The authors are deeply indebted to the Assiut University Mycological Centre, Assiut University for the financial support provided.

AUTHOR'S CONTRIBUTION

All authors shared in the experimental designed and assisted in the work, formatting the tables, interpretation of data and in preparation and editing of the manuscript. The final manuscript has been approved by all authors.

TRANSPARENCY DECLARATION

The authors declare that there is no conflict of interest regarding the publication of this article.

REFERENCES

1. Johnson LF, Curl EA. Methods for research on the ecology of soil-borne plant pathogens. Burgess Publishing Company, Minneapolis, 1972.
2. Moubasher AH, Abdel-Sater MA, Soliman Z. Biodiversity and molecular characterization of yeast and filamentous fungi in the air of citrus and grapevine plantations in Assiut area, Egypt. *Mycosphere*. 2016; 7(3): 236-261.
3. Shear CL, Dodge BO. Life histories and heterothallism of the red bread-mold fungi of the *Monilia sitophila* group. *J Agricult Res*. 1927; 34: 1019-1042.
4. Cain RF. Studies of coprophilous ascomycetes. I. *Gelasinospora*. *Can J Res*. 1950; 28: 566-576.
5. von Arx JA. A key to the species of *Gelasinospora*. *Persoonia*. 1982; 11: 443-449.
6. Garcia D, Stchigel AM, Cano J, Guarro J, Hawksworth DL. A synopsis and re-circumscription of *Neurospora* (syn. *Gelasinospora*) based on ultrastructural and 28S rDNA sequence data. *Mycol Res*. 2004; 108(10): 1119-1142.
7. Tai FL. Two new species of *Neurospora*. *Mycologia*. 1935; 27: 328-330.
8. Gochenaur SE, Backus MP. A new species of *Neurospora* from Wisconsin lowland soil. *Mycologia*. 1962; 54: 555-562.
9. Nelson AC, Novak RO, Backus MP. A new species of *Neurospora* from soil. *Mycologia*. 1964; 56: 384-392.
10. Frederick LF, Ueher FA, Benjamin CP. A new species of *Neurospora* from soil of West Pakistan. *Mycologia*. 1969; 61: 1077-1084.
11. Mahoney DP, Huang LH, Backus MP. New homothallic *Neurosporas* from tropical soils. *Mycologia*. 1969; 61: 264-272.
12. von Arx JA. The genera of fungi sporulating in pure culture. J. Cramer, Vaduz, 3rd edn, 1981.
13. Perkins DD, Raju NB. *Neurospora discreta*, a new heterothallic species defined by its crossing behaviour. *Exp Mycology*. 1986; 10: 323-338.
14. Krug JC, KHAN RS. A new homothallic species of *Neurospora* from Hungary. *Mycologia*. 1991; 83: 829-832.

15. Dowding ES. *Gelasinospora*, a new genus of Pyrenomyces with pitted spores. Can J Res. 1933; 9: 294-305.
16. Moreau C, Moreau M. Quelques ascomycetes du Congo. Revue de Mycologie. 1949; 2: 50-66.
17. Udagawa S, Takada M. Notes on some Japanese ascomycetes. Transact Mycol Soc Japan. 1967; 8: 50-53.
18. Cailleux R. Recherches sur la mycoflore coprophile centrafricaine. Le genres *Sordaria*, *Gelasinospora*, *Bombardia*. Bull Soc Mycol France. 1971; 87: 461-626
19. Udagawa S, Furuya K, Horie Y. Mycological reports from New Guinea and the Solomon Islands. 19. Notes on some ascomycetous microfungi from soil. Bull Nat Sci Museum Tokyo. 1973; 16: 503-520.
20. Horie Y, Udagawa S. *Anixiella* and *Gelasinospora* from Himalayan soils. Transact Mycol Soc Japan. 1974; 15: 196-205.
21. Furuya K, Udagawa S. New species of *Gelasinospora* and *Anixiella*. Transact Mycol Soc Japan. 1976; 17: 313-320.
22. Khan RS, Krug JC. New species of *Gelasinospora*. Mycologia. 1989; 81: 226-233.
23. Khan RS, Krug JC. A new terricolous species of *Gelasinospora*. Sydowia. 1989; 41: 180-184.
24. Krug JC, Khan RS, Jeng RS. A new species of *Gelasinospora* with multiple germ pores. Mycologia. 1994; 86: 250-253.
25. Stchigel AM, Cano J, Guarro J. A new species of *Gelasinospora* from Argentinian soil. Mycol Res. 1998; 102: 1405-1408.
26. Dettman JR, Harbinski FM, Taylor JW. Ascospore morphology is a poor predictor of the phylogenetic relationships of *Neurospora* and *Gelasinospora*. Fungal Gen Biol. 2001; 34: 49-61.
27. Cai L, Jeewon R, Hyde KD. Phylogenetic investigations of Sordariaceae based on multiple gene sequences and morphology. Mycol Res. 2006; 110: 137-150.
28. Moharram AM, Bagy MMK, Abdel-Mallek AY. Saprophytic fungi isolated from animal and bird pens in Egypt. J Basic Microbiol. 1987; 27(7): 361-367.
29. Moharram AM, Abdel-Gawad KM, Megalla SE, Mahmoud A-LE. Fungal flora of poultry feedstuff ingredients. J Basic Microbiol. 1989; 29(8): 491-499.
30. Abdel-Hafez SII, Moubasher AH, Shoreit AAM, Ismail MA. Fungal flora associated with combine harvester wheat and sorghum dusts from Egypt. J Basic Microbiol. 1990; 30(7): 467-479.
31. Abdel-Mallek AY, Abdel-Hafez AII, Moharram AM. Contribution to the mycoflora of caraway, coriander and cumin seeds in Egypt. Bull Faculty Sci Assiut Univ. 1990; 19(1-D): 1-15.
32. Ismail MA, Abdel-Hafez SII, Moharram AM. Aeromycobiota of western desert of Egypt. Afr J Sci Technol. 2002; 3(1): 1-9.
33. Abdel-Sater MA, Moubasher AH, Soliman ZSM. Biodiversity of filamentous and yeast fungi in soil of citrus and grapevine plantations in Assiut area, Egypt. Czech Mycol. 2016; 68(2): 183-214.
34. Moubasher AH, Moharram AM, Soliman Z. Contributions to the mycobiota of Egypt: *Neurospora tetrasperma* Shear & Dodge; a new record to Egypt. J Basic Appl Mycol Egypt. 2010; 1: 67-70.
35. Samson RA, Hoekstra ES, Frisvad JC. Introduction to food- and airborne fungi. 7th edn. Centraalbureauvoor Schimmelcultures, Utrecht, The Netherlands, 2004.
36. Thompson JD, Higgins DG, Gibson TJ. CLUSTAL W: Improving the sensitivity of progressive multiple sequence alignment through sequence weighting, position-specific gap penalties and weight matrix choice. Nucleic Acids Res. 1994; 22: 4673-4680.
37. Ginns JH. Compendium of plant disease and decay fungi in Canada 1960-1980. Agricultur Canada, Ottawa, 1986.
38. Lumley TC, Abbott SB, Currah RS. Microscopic ascomycetes isolated from rotting wood in the Boreal forest. Mycotaxon. 2000; 74(2): 395-414.
39. Geydan TD, Debets AJ, Verkley GJ, van Diepeningen AD. Correlated evolution of senescence and ephemeral substrate use in the Sordariomycetes. Mol Ecol. 2012; 21(11): 2816-2828.
40. Wang XW, Lombard L, Groenewald JZ, Li J, Videira SI, Samson RA, et al. Phylogenetic reassessment of the *Chaetomium globosum* species complex. Persoonia. 2016; 36: 83-133.

The relevance of sebum composition in the etiopathogeny of acne

Marisa Gonzaga da Cunha¹, Francisca Daza¹, Carlos D. Aparecida Machado Filho¹,
Glaucia Luciano da Veiga², Fernando Fonseca^{1-3*}

¹ Dermatology Discipline, Faculdade de Medicina do ABC, Santo André, São Paulo, Brazil

² Clinical Analysis Department, Faculdade de Medicina do ABC, Santo André, São Paulo, Brazil

³ Pharmaceutical Sciences Department, Universidade Federal de São Paulo, Diadema, São Paulo, Brazil

*Corresponding author: Fernando Luiz Affonso Fonseca; Faculdade de Medicina do ABC, Lauro Gomes Avenue, 2000, Santo André, São Paulo, Zip Code 09060-650, Brazil; Phone: +551149935488 ; E-mail: profferfonseca@gmail.com

Received: 08 January 2018; **Revised submission:** 15 February 2018; **Accepted:** 23 February 2018

Copyright: © The Author(s) 2018. European Journal of Biological Research © T.M.Karpiński 2018. This is an open access article licensed under the terms of the Creative Commons Attribution Non-Commercial 4.0 International License, which permits unrestricted, non-commercial use, distribution and reproduction in any medium, provided the work is properly cited.

DOI: <http://dx.doi.org/10.5281/zenodo.1184139>

ABSTRACT

Acne vulgaris is an inflammatory disease that develops around the hair follicle. Many are the interconnected etiopathogenic factors involved, among which we can mention the increase in levels of androgen hormones, sebum hypersecretion, follicular hyperkeratosis with microcomedo formation, the proliferation of the bacteria *Propionibacterium acnes* (*P. acnes*) and the resulting inflammatory response. The way this bacterial growth occurs and how it is connected with the development of the inflammatory process have been themes of many clinical and experimental trials. Modifications in the sebum composition lead to a greater proliferation and differentiation of keratinocytes that obstruct the follicular ostium and favor the formation of comedones. On the other hand, these modifications alter the follicular hydration and facilitate the proliferation of the *P. acnes*, which not only produces chemotactic factors but also releases lipase that oxidizes the squalene. The oxidized squalene induces the formation of pro-inflammatory cytokines and boosts the innate immunity of keratinocytes and sebocytes, thus

generating the inflammatory process. The aim of this study was to review the literature regarding the new concepts on the pathogenesis of acne.

Keywords: Acne; Sebum composition; Review.

1. INTRODUCTION

Acne vulgaris, with its many etiopathogenic factors involved, is a primary inflammatory pathology of the skin [1]. The induction of the inflammatory signaling in the pilosebaceous unit is an essential component in the developing process of the lesions [2, 3]. It commonly starts during puberty with the increase of androgen production, resulting in the increase of sebum production. The overproduction of the latter, associated with the abnormal shedding of keratinocytes, lead to the obstruction of the follicle opening and the formation of microcomedones [4].

The sebum accumulation in the follicular infundibulum stimulates the proliferation of the Gram-positive bacteria *Propionibacterium acnes* (*P. acnes*) in genetically predisposed individuals [5]. This increase in the bacterial population leads to the

release of not only cytokines such as interleukins IL-6 and IL-8 by the infundibular keratinocytes, but also IL-8, IL-12 and pro-inflammatory mediators by the macrophages, resulting in the development of the inflammation in the follicle and in the adjacent dermis [3].

Therefore, the key factors involved in the pathogenesis of acne are classically established as follows:

- (1) increase in levels of androgen hormones,
- (2) sebum hypersecretion,
- (3) follicular hyperkeratosis with microcomedo formation,
- (4) the proliferation of the bacteria *Propionibacterium acnes* (*P. acnes*), and
- (5) the resulting inflammatory response [4, 5].

The way this bacterial growth occurs and how it is connected with the development of the inflammatory process have been themes of many clinical and experimental trials, which have revealed the relation of the production of pro-inflammatory cytokines by the sebocytes and keratinocytes with the quantitative and qualitative variations of the lipid content of the sebum caused by the *P. acnes* in particular [3-6]. Some studies suggest that the deregulation in the sebum production along with the alterations in its composition play an essential role in the abnormal follicular proliferation and in the development of the inflammation that triggers comedonal lesions [7, 8].

Thus, the aim of this study was to review the literature regarding the new concepts on the pathogenesis of acne.

2. THE ROLE OF SEBUM IN THE PROLIFERATION OF *P. ACNES*

Human sebum is a holocrine secretion formed by the disintegration of sebocytes. It is composed of a nonpolar mixture which contains triglycerides (41%), free fatty acids (16%), squalene (12%), monoester waxes (25%), cholesterol ester and free cholesterol (4%) and vitamin E [6, 9]. Squalene participates in the antioxidant defense system of the skin by suppressing oxidized free radicals. Furthermore, it plays an important role not only in anti-inflammatory actions but also in the development of acne [10, 11].

On the cutaneous surface microorganisms and

oxygen transform the sebum produced by the glands. In normal skin, through the lysis of triglycerides, the formation of fatty acids occurs. The linoleic acid is one of them, which besides being the main constituent of acyl-glucosylceramides, acylceramides and acyclic lipids also contributes to the stratum corneum hydration and the integrity of the cutaneous barrier [10, 11]. Sebum lipids also promote photoprotection, especially against UVB irradiation, and they have lipophilic antioxidants. Linoleic acid is also directly related to the synthesis of squalene and monoester waxes [6, 9, 12]. Cutaneous surface lipids, especially those secreted by the sebaceous glands and transported through the follicular duct, are part of the skin innate immunity and contribute to the antimicrobial skin barrier, thus limiting bacterial colonization [6].

Recent studies have revealed that in patients with acne the amount of linoleic acid in the sebum is reduced, affecting the composition of sphingolipids in the follicle, which is associated with the increase in concentration of the sebaleic acid and squalene [12]. The greater permeability of the stratum corneum, resultant from the reduction in the linoleic acid levels and the consequent reduction in the sphingolipid generation, increases follicular hydration, which allows for the proliferation of the *P. acnes* in the comedo. In turn, it generates lipase, which plays an important role in the alteration of the lipid composition of the sebum [5, 13].

3. MODIFICATION OF THE SEBUM COMPOSITION AND THE INFLAMMATION

It has been demonstrated that, besides hyperseborrhea, lipid peroxidation and alterations in the lipid composition of the sebum, which are caused by the proliferation of the *P. acnes* and defined as disseborrhea, are essential etiopathogenic factors in the acne process. Such factors play a key role in the induction of the inflammation and in comedogenesis [14]. Moreover, low levels of linoleic acid also lead to an alteration in the cutaneous barrier function due to the increase in the permeability of the comedo wall to inflammatory substances [3].

The accumulation of peroxidized lipids, especially peroxidized squalene, can induce the production of the pro-inflammatory cytokines IL-1 α , IL-6 and IL-8 as well as the activation of

peroxisome proliferator-activated receptors (PPARs), which are nuclear transcription factors involved in the control of lipid metabolism and the control of the inflammation [9, 15, 16]. This accumulation in the comedones is positively correlated to the grading of acne severity [17, 18].

Keratinocytes and sebocytes also act as immune active cells since innate immunity molecules, like toll-like receptors TLR-2 and TLR-4, CD1 and CD14, are expressed in human keratino-

cytes. Besides, antimicrobial peptides, like defensin 1, defensin 2 and cathelicidin, are also expressed and they can be activated in the sebaceous gland. Such molecules can be activated by the *P. acnes* and by the altered lipid content in the sebum, thus producing pro-inflammatory cytokines through the activation of nuclear transcription factor (NF), which, in turn, can induce lipogenesis (Figure 1) [3, 7].

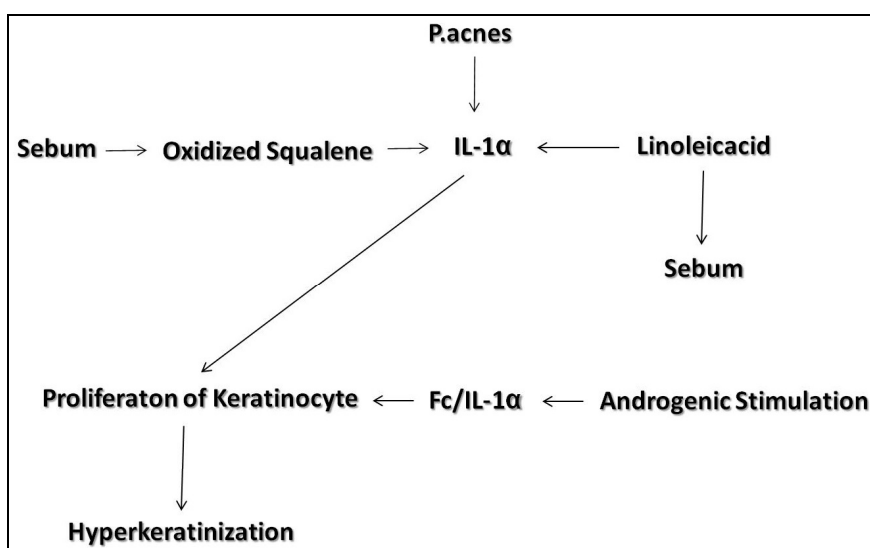


Figure 1. Representative scheme of the triggering of the inflammatory process. Adapted from Reynolds [7].

Prostaglandins are other pro-inflammatory mediators thought to be involved in the acne lesion development [19]. Studies conducted with rats revealed that the increase in the expressions of cyclooxygenase-2 (COX-2) and prostaglandin E2 (PGE2) induces hyperplasia of the sebum glands and an increase in sebum production [20].

Other studies have also shown the relation between the modifications in the sebum composition due to oxidation and the progression of the inflammatory condition. The concentration of peroxidized lipids and IL-1 α is significantly higher in the comedones when compared with the concentration in the stratum corneum, which is determined/explained by the proliferation of the existing bacterial flora and the *P. acnes* in the comedo. Such proliferation leads to the rupture of the glandular wall with the propagation of the inflammatory reaction in the dermis and in the dermal vascular component/network. *P. acnes* stimulates the secre-

tion of the comedogenic cytokine IL1- α , which, besides playing a critical role in the pathogenesis of acne, also stimulates vascular endothelial cells to produce inflammatory markers [8, 9, 20], thus aggravating the clinical condition.

4. MODIFICATION OF THE SEBUM AND FOLLICULAR HYPERKERATOSIS

Recent studies have shown that the amount of linoleic acid in the sebum is reduced in patients with acne, thus affecting the composition of the sphingolipids in the follicle [9, 12, 14]. The abnormal distribution of fatty acids affects the proliferation and differentiation of keratinocytes, with the resultant development of follicular hyperkeratosis and the comedo [12].

On the other hand, the relation between oxidized lipids and antioxidants on the surface of the skin has been considered of extreme importance in

the etiopathogenesis of the acne. Some components of this complex mixture of molecules are clearly cytotoxic or irritating, and they cause a reactive follicular hyperkeratosis. Again, the accumulation of peroxidized lipids, especially peroxidized squalene, can induce not only the production of pro-inflammatory cytokines but also the activation of PPARs. The enzymes involved in the expression/formation of the PAARs, including 5-LOX, have been related to inflammatory disease of the skin characterized by the hyperproliferation of keratino-

cytes [3, 7, 10].

Therefore, the inflammatory process triggered by lipid peroxidation seems to be the promoting factor of abnormal keratinization and comedogenesis [19]. Some studies in animals show that peroxidized squalene induces epithelial hyperkeratosis in the follicular infundibulum and sebaceous hyperplasia in the ears of rats and rabbits [21, 22]. Furthermore, patients with acne have increased levels of IL-1 α in the stratum corneum, with higher concentrations in comedogenic areas (Figure 2) [18].

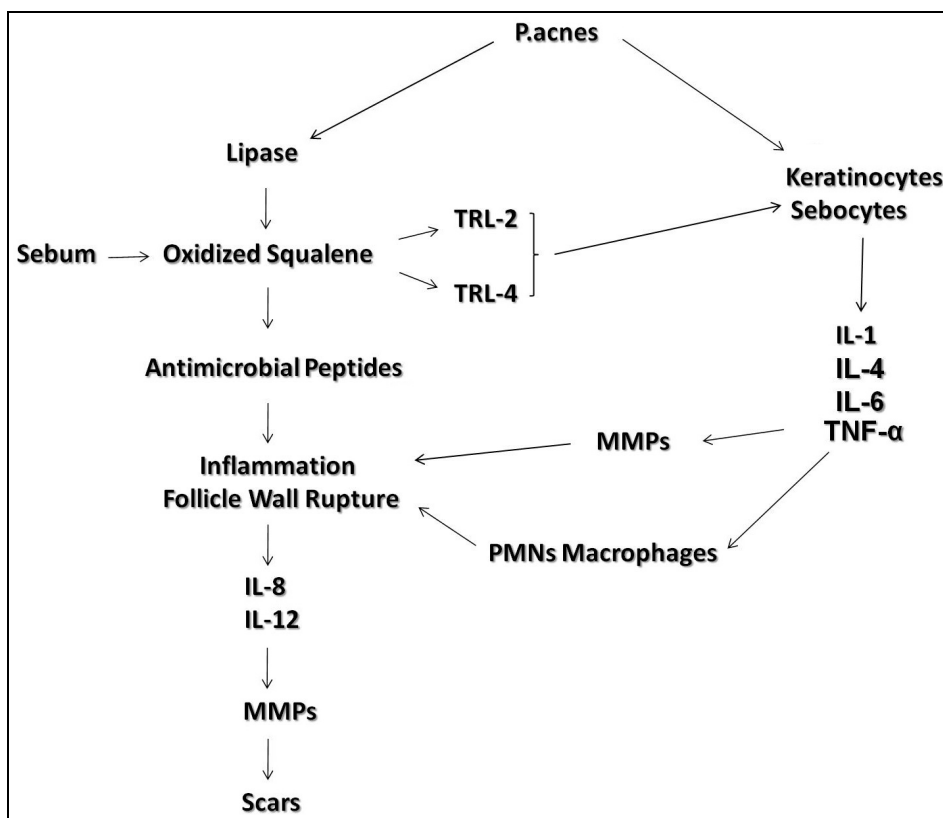


Figure 2. Representative scheme of the process of hyperkeratinization.

5. CONCLUSION

The linoleic acid reduction promotes a greater proliferation and differentiation of keratinocytes that obstruct the follicular ostium and favor the formation of comedones. On the other hand, this reduction alters the follicular hydration and facilitates the proliferation of the *P. acnes*, which not only produces chemotactic factors but also releases lipase that oxidizes the squalene. The oxidized squalene induces the formation of pro-inflammatory cytokines and boosts the innate immu-

nity of keratinocytes and sebocytes, thus generating the inflammatory process.

In conclusion, through many distinct mechanisms, the resulting compounds of sebum oxidation play a fundamental role both in the pathogenesis as well as in the maintenance of the inflammatory process of the acne.

AUTHORS' CONTRIBUTION

MGC: Conception and design, Development of methodology, Acquisition of data, Administrative,

technical, or material support. FD: Acquisition of data, Analysis and interpretation of data, Administrative, technical, or material support. CDAMF: Acquisition of data. GLV: Writing, review and/or revision of the manuscript. FF: Study supervision, Analysis and interpretation of data, Writing, review and/or revision of the manuscript. The final manuscript has been approved by all authors.

TRANSPARENCY DECLARATION

The authors declare that there is no conflict of interest regarding the publication of this article.

REFERENCES

- Leon H, Kircik MD. Advances in the understanding of the pathogenesis of inflammatory acne. *J Drugs Dermatol*. 2016; 15: s7-s10.
- Jeremy AH, Holland DB, Roberts SG, Thomson KF, Cunliffe WJ. Inflammatory events are involved in acne lesions initiation. *J Invest Dermatol*. 2003; 121: 20-27.
- Zouboulis CC, Jourdan E, Picardo M. Acne is an inflammatory disease and alterations of sebum composition initiate acne lesions. *JEADV*. 2014 28: 527-532.
- Cunha MG, Fonseca FLA, Machado CA. Androgenic hormone profile of adult women with acne. *Dermatology*. 2013; 226: 167-171.
- Tilles G. Acne pathogenesis: history of concepts. *Dermatology*. 2014; 229: 1-46.
- Picardo M, Ottaviani M, Camera E, Mastrofrancesco A. Special focus review - sebaceous gland lipids. *Dermato-Endocrinol*. 2009; 1(2): 68-71.
- Das S, Reynolds RV. Recent advances in acne pathogenesis: implications for therapy. *Am J Clin Dermatol*. 2014; 15: 479-488.
- Kang S, Cho S, Chung JH, Hammerberg C, Fisher GJ, Voorhees JJ. Inflammation and extracellular matrix degradation mediated by activated transcription factors nuclear factor- κ band activator protein-1 in inflammatory acne lesions in vivo. *Am J Pathol*. 2005; 166: 1691-1699.
- Ottaviani M, Camera E, Picardo M. Lipid mediators in acne. *Mediators Inflamm*. 2010; 2010: 858176.
- Saint-Leger D, Bague A, Lefebvre E, Cohen E, Chivot M. A possible role for squalene in the pathogenesis of acne. II. In vivo study of squalene oxides in skin surface and intra-comedonal lipids of acne patients. *Br J Dermatol*. 1986; 114: 543-552.
- Thiboutot D. Regulation of human sebaceous glands. *J Invest Dermatol*. 2004; 123: 1-12.
- Stewart ME, Grahek MO, Cambier LS, Wertz PW, Downing DT. Dilutional effect of increased sebaceous gland activity on the proportion of linoleic acid in sebaceous wax esters and in epidermal acylceramides. *J Invest Dermatol*. 1986; 87: 733-736.
- Pappas A, Johnsen S, Liu JC, Eisinger M. Sebum analysis of individuals with and without acne. *Dermato-Endocrinology*. 2009; 1(3): 157-161.
- Bickers DR, Athar M. Oxidative stress in the pathogenesis of skin disease. *J Invest Dermatol*. 2006; 126: 2565-2575.
- Niki E. Lipid oxidation in the skin. *Free Radical Res*. 2015; 49: 827-834.
- Capitanio B, Lora V, Ludovici M, Sinagra JL, Ottaviani M, Mastrofrancesco A, et al. Modulation of sebum oxidation and interleukin-1 α levels associates with clinical improvement of mild comedonal acne. *J Eur Acad Dermatol Venereol*. 2014; 28: 1792-1797.
- Ottaviani M, Alestas T, Flori E, Mastrofrancesco A, Zouboulis CC, Picardo M. Peroxidated squalene induces the production of inflammatory mediators in HaCaT keratinocytes: a possible role in acne vulgaris. *J Invest Dermatol*. 2006; 126: 2430-2437.
- Pham DM, Bousouira B, Moyal D, Nguyen QL. Oxidation of squalene, a human skin lipid: a new and reliable marker of environmental pollution studies. *Int J Cosmet Sci*. 2015; 37: 357-365.
- Mills OH, Criscito MC, Schlesinger TE, Verdicchio R, Szoke E. Addressing free radical oxidation in acne vulgaris. *J Clin Aesthet Dermatol*. 2016; 9: 25-30.
- Neufang G, Fürstenberger G, Heidt M, Marks F, Müller-Decker K. Abnormal differentiation of epidermis in Transgenic mice constitutively expressing cyclooxygenase-2 in skin. *Proc Natl Acad Sci USA*. 2001; 98: 7629-7634.
- Chiba K, Yoshizawa K, Makino I, Kawakami K, Onoue M. Comedogenicity of squalene monohydroperoxide in the skin after topical application. *J Toxicol Sci*. 2000; 25: 77-83.
- Motoyoshi K. Enhanced comedo formation in rabbit ear skin by squalene and oleic acid peroxides. *Br J Dermatol*. 1983; 109: 191-198.

Antioxidant potential of the farmer preferred selections of *Solanum aethiopicum* vegetable consumed in central Uganda

S. Sekulya¹, A. Nandutu^{1*}, A. Namutebi², J. Ssozi², M. Masanza³, B. Kabod³,
J. N. Jagwe⁴, A. Kasharu⁵, D. Rees⁶, E. B. Kizito³

¹ Department of Biochemistry, College of Natural Sciences, Makerere University, Uganda

² Department of Food Technology and Nutrition, College of Agricultural and Environmental Sciences, Makerere University, Uganda

³ Department of Agricultural and Biological Sciences, Faculty of Science and Technology, Uganda Christian University, Uganda

⁴ Farmgain Africa Limited, Plot 1 Kimera Road, 2nd Floor Ntinda Shopping Mall P.O. Box 21717 Kampala, Uganda

⁵ Coalition for Health Agricultural Income Networks, Plot 115, Busega, Kampala - Masaka, Uganda

⁶ Natural Resources Institute, University of Greenwich, Central Avenue, Chatham Maritime, Chatham, Kent ME4 4TB, UK

*Corresponding author: A. Nandutu; E-mail: anandutu@cns.mak.ac.ug

Received: 11 December 2017; Revised submission: 10 February 2018; Accepted: 05 March 2018

Copyright: © The Author(s) 2018. European Journal of Biological Research © T.M.Karpiński 2018. This is an open access article licensed under the terms of the Creative Commons Attribution Non-Commercial 4.0 International License, which permits unrestricted, non-commercial use, distribution and reproduction in any medium, provided the work is properly cited.

DOI: <http://dx.doi.org/10.5281/zenodo.1195552>

ABSTRACT

In addition to the rich micronutrient value, indigenous vegetables are regarded as possessing medicinal attributes. The Solanaceae family has over 1000 species worldwide, with a number of indigenous species originating in Africa. The most popular leafy vegetable in Uganda is the *Solanum aethiopicum* (Nakati). The objective of this study was to determine the selected phytochemical attributes, chlorophyll content, moisture content and total antioxidant activity of the farmer preferred selections within the landraces of *Solanum aethiopicum* leafy vegetable in Uganda. The antioxidant activity was achieved by screening the leaf extracts for their free radical scavenging properties using diphenyl picryl hydrazyl (DPPH) and ascorbic acid as standard. The ability of the extracts to scavenge DPPH radical was determined spectrophotometrically at 517 nm. The study showed

that all the landraces had a high polyphenol and flavonoid content with SAS185/P/2015 containing the highest flavonoid content (3.16±0.06 mg QE/g fw). SAS1641/2015 showed the highest total polyphenol content of 7.79±0.27 mg GAE/g fw and also showed the highest vitamin C content. This contributed to the high total antioxidant activity of 2.79±0.01 and 5.43±0.02 mg AAE/g fw when using FRAP and DPPH methods respectively. SAS145/2015 presented the highest chlorophyll content of 19.69±0.01 mg/g dwb. All the landraces showed a high percentage moisture content that ranged from 82.66±0.35 to 84.21±0.48%. These results are of nutraceutical significance and hence confirm their usage as medicinal vegetables.

Keywords: Landraces; Polyphenols; Flavonoids; Vitamin C; Total antioxidant activity; Ferric reducing antioxidant power (FRAP); Diphenyl-picrylhydrazyl (DPPH).

1. INTRODUCTION

Consumption of fruits and vegetables has attracted growing interest because many epidemiological and biochemical studies have consistently demonstrated a clear and significant positive association between intake of these natural food products, and reduced rates of chronic diseases such as heart disease, common cancers, degenerative diseases and as well as aging [1]. The protection that fruits and vegetables provide against these maladies is attributed to the presence of several antioxidants such as ascorbic acid (vitamin C), α -tocopherol (vitamin E) and β -carotene (provitamin A) [1, 2] and polyphenolic substances [1].

Vegetables in Uganda are mostly grown by small scale farmers at subsistence levels. There are over 600 local vegetable species in Uganda [3]. These vegetables are perishable and low yielding and their commercial value has not yet been well explored. The traditional vegetables have very high nutritious value [4] for example they are rich in β -carotene, vitamins E and C, proteins and minerals such as iron, calcium, phosphorus, iodine and fluorine. Most traditional vegetables have medicinal value for example *Solanum indicum* (Katunkuma) is used to control high blood pressure, *Amaranthus dubius* (dodo) and *Amaranthus lividus* (ebuga) are also believed to increase blood levels [3, 5]. The consumption of vegetables has been known to alleviate micronutrient malnutrition which is the cause of chronic diseases [5]. The most common traditional vegetables grown especially in central Uganda include *Amaranthus dubius*, *A. lividus*, *A. blitum* (Ebugga eryanamusayi); *Solanum aethiopicum* (Nakati); *S. gilo* (Entula enganda); *S. indicum* subsp. *distichum* or *S. anguivi* (Katunkuma); *S. nigrum* (Ensugga enzirugavu); and *Gynandropsis (Cloeme) gynandra* (Ejjobyo) [3]. These leafy vegetables are used as side-dish accompanying the thick starchy meals [5]. Only a few of these vegetables are commercially grown.

There are over 1000 species of the Solanaceae family out of which 100 indigenous species are in Africa [6] and several studies have supported the use of these vegetables as foods and medicinal preparations [6]. Despite these benefits from vegetables and the nutrients they contain, there has been limited research on local vegetable varieties in

Uganda [3]. Of the commonly grown vegetable varieties, *Gynandropsis (Cloeme) gynandra*, *Amaranthus dubius*, *A. lividus*, *A. blitum* and *Solanum aethiopicum* are grown by a larger number of farmers and ranked higher than the others, for both food and cash. *Solanum aethiopicum* is the most commonly grown leafy vegetable in Uganda. Within this vegetable, there are several landraces which differ in stem color, leaf color (with different shades of green), leaf margin structure, leaf size and stem height at market maturity. Farmers in Uganda prefer *Solanum aethiopicum* with broad leaves, 1.5 feet height at market maturity and that with strong green color. These differences may be due to genetics and environmental factors. Due to the differences, there is expected difference in the phytochemical attributes within the landraces. Many of these selections are mainly consumed for their nutritional values and the acceptability of these vegetables depends on texture and appearance that depends on the chlorophyll content [7] without much consideration for their therapeutic importance. Few vegetables in Uganda have been explored for phytochemical and antioxidant activity studies. The objective of this study was therefore to determine the selected phytochemical attributes, total antioxidant activity, vitamin C, chlorophyll and moisture content of the farmer preferred selections within the landraces of *Solanum aethiopicum* leafy vegetable.

2. MATERIALS AND METHODS

2.1. Chemicals and reagents

The chemicals and reagents used included: methanol, Folin-Ciocalteu, sodium hydrogen carbonate, gallic acid, aluminium chloride, Na-K tartarate, quercetin, diphenylpicrylhydrazyl, 2,4,6-tri(2-pyridyl)-s-triazine, iron(III) chloride, ascorbic acid, metaphosphoric acid, glacial acetic acid, 2,4-dinitrophenyl hydrazine, hydrochloric acid, ammonium thiocyanate and acetone. They were all of analytical grade and purchased from Sigma Germany. The filter papers were purchased from Whatman UK.

2.2. Sample treatment

The screened landraces were collected from

the Uganda Christian University Agricultural research Farm in Ntawo, Mukono district, central Uganda. The whole *S. aethiopicum* plants were uprooted, shaken to remove soil and wrapped in aluminium foil, put in a cooler box and transported to the research laboratory of the Food Technology and Nutrition department of the college of Agricultural and Environmental sciences, Makerere University, Uganda. The edible parts of the plant (leaves) were removed and washed with running water and used for extraction to determine content of selected phytochemicals and total antioxidant activity except for samples used for moisture content determination which were not washed.

2.3. Preparation of extracts

The extraction was done according to the method previously described by Wissam et al. [8] but with modification. The edible parts of fresh leaves were blended and 1 g of powdered sample dissolved in 50 ml of 80% methanol solution in a conical flask placed in a thermostatic water bath shaker at 45°C for 20 minutes. The liquid extract was separated from solids by centrifugation at 2000 rpm for 10 minutes and the supernatant stored at -20°C. This extraction was done in triplicates.

2.4. Determination of polyphenol content

The total phenolic content was determined by Folin-Ciocalteu's method [9]. This was done by measuring 0.5 ml of extract, and adding 2.5 ml of 10% Folin-Ciocalteu's reagent dissolved in water, followed by 2.5 ml of 7.5% NaHCO₃, incubated at room temperature in the dark for 45 minutes and absorbance was determined at 765 nm. The samples were prepared in triplicate for each analysis and mean values of absorbance obtained. The standard solutions of gallic acid of concentrations 0.01, 0.02, 0.03, 0.04, 0.05 mg per ml were used to construct a standard calibration curve [10] and the concentration of phenolics were determined in mg per g of fresh sample.

2.5. Determination of flavonoids content

The flavonoid content was determined using the aluminium chloride method [11]. To the aliquots

of extract solution made up to 3 ml with methanol, 0.1 ml of 10% AlCl₃ solution, 0.1 ml Na-K tartarate and 2.8 ml of distilled water was added sequentially and mixture shaken vigorously and incubated for 30 minutes at room temperature in the dark and absorbance determined at 415 nm using Genesys 10-UV spectrophotometer (Thermo Electron Corporation, Madison WI, USA). Known concentrations of quercetin, 0.01, 0.02, 0.03, 0.04, 0.05 mg per ml were used to generate a standard calibration curve for absorbance at 415 nm. Then concentration of flavonoids calculated from calibration curve and expressed as mg quercetin equivalent per g of fresh sample.

2.6. Determination of antioxidant activity

2.6.1. Free radical scavenging activity by the DPPH method

The free radical scavenging activity was assayed using free radical scavenging activity via DPPH method as previously described [12]. DPPH stock solution (1M) in methanol was prepared and kept at -20°C and a 0.1 mM DPPH was used for the test which was prepared by diluting 10 ml of the stock solution with 90 ml of methanol. Ascorbic acid was used as the standard prepared with concentrations of 25, 50, 75, 100 and 125 µg/ml. Equal volumes of 1.5 ml of the standard and the sample was added and kept in the dark for 30 minutes and absorbance measured at 517 nm using Genesys 10-UV spectrophotometer (Thermo Electron Corporation, Madison WI, USA). The percentage inhibition of both standard and samples calculated.

$$\% \text{ inhibition} = [(AB - AA) / AB] \times 100$$

AB is absorbance of control sample and AA is absorbance of sample.

A calibration curve was obtained by plotting % inhibition against ascorbic acid concentration. The results were expressed as ascorbic acid equivalent in mg/g of fresh sample.

2.6.2. Radical scavenging activity by FRAP method

Ferric reducing antioxidant power assay was performed using the method as previously described but with modifications [13]. To the extract (1 ml)

was added with 1 ml of FRAP reagent, that was prepared with mixture of 300 mM sodium acetate buffer (pH 3.6), 10 mM 2,4,6-tri(2-pyridyl)-s-triazine (TPTZ) solution and 20 mM $\text{FeCl}_3 \cdot 6\text{H}_2\text{O}$ in a ratio of 10:1:1, and diluted with water to a total volume of 4 ml. The reaction mixture was incubated in a water bath at 37 °C for 30 minutes and absorbance determined at 593 nm using Genesys 10-UV spectrophotometer (Thermo Electron Corporation, Madison WI, USA). Ascorbic acid was used as the standard prepared with concentrations of 25, 50, 75, 100 and 125 µg/ml. The results were expressed as ascorbic acid equivalent in mg per g of fresh sample.

2.7. Vitamin C analysis

Extraction method for vitamin C extraction was done using 5% metaphosphoric acid - 10% acetic acid solution [14]. The fresh leaves of vegetable were blended and to 10 g of the blended sample, 50 ml of 5% metaphosphoric acid - 10% acetic acid solution added and mixture transferred into a 100 ml volumetric flask and shaken gently until a homogeneous dispersion is obtained. The mixture was diluted to the mark with 5% metaphosphoric acid - 10% acetic acid solution. The resultant mixture was filtered using Whatman No. 1 filter paper and filtrate used to determine the total Vitamin C in the sample. This was repeated every after 24 hours for seven days for every postharvest handling method. The extraction was done in triplicates. The total vitamin C was determined using UV-spectrophotometer [14]. Excess bromine water was added to 1 ml of extract (bromine oxidizes ascorbic acid to dehydroascorbic acid), 3 drops of thiourea were added to remove excess bromine to form a colorless solution followed by 1 ml of 2,4-dinitrophenyl hydrazine to form an osazone and mixture incubated at 37°C for 3 hours in a water bath. The mixture was finally cooled in an ice bath and 5 ml of 85% sulphuric acid added with constant stirring to obtain a red colored complex and absorbance determined at 521 nm using Genesys 10-UV spectrophotometer (Thermo Electron Corporation, Madison WI, USA). A 0.5 mg/ml solution of L-ascorbic acid stock solution was prepared and used to prepare different standard solutions of ascorbic acid which were used to

develop a standard curve from which the vitamin C concentrations in the leaves was determined.

2.8. Determination of chlorophyll

The chlorophyll was extracted with acetone and determined using a UV Vis spectrophotometer [15]. Accurately weighted 0.1 g of fresh leaf sample was taken, and macerated in 10 ml of 80% acetone solution as extracting solvent using celite. The mixture was then filtered using Whatman No 1 filter paper and filtrate diluted with 80% acetone. The solution mixture was then analyzed for Chlorophyll-a and Chlorophyll-b content in a UV-spectrophotometer at 663.2 nm and 646.8 nm respectively using Genesys 10-UV spectrophotometer (Thermo Electron Corporation, Madison WI, USA). The quantification of chlorophyll a and b was done using the equation described shown below and results expressed in mg/g dwb.

$$\text{Cha} = 12.25A_{663.2} - 2.79A_{646.8}$$

$$\text{Chb} = 21.5A_{646.8} - 5.1A_{663.2}$$

2.9. Determination of moisture content

The moisture content of the samples was determined as previously described [16]. A thoroughly washed Petri-dish was placed in the oven to dry and then weighed. The blended sample (3 g) was then placed in the weighed Petri dish, and then placed in an oven to dry at 60°C for 16 hours. The dish and dry sample were transferred to a desiccator to cool at room temperature before being weighed again. Every sample was analyzed in triplicate.

2.10. Statistical analysis

The results were reported as the mean and standard deviation. Analysis of variance (ANOVA) was applied to the data using SPSS version 16.0 for windows (SPSS, Inc., Chicago, IL, USA). The significant differences were obtained using the Tukey HSD test ($p \leq 0.05$) and correlation coefficients between antioxidant components and antioxidant activity were determined.

3. RESULTS

3.1. Total polyphenols and flavonoids content

The total flavonoid content was ranging from 1.91 ± 0.16 to 3.16 ± 0.06 mg/g fw of fresh sample. There was a significant difference ($P \leq 0.05$) in the flavonoid content among the six landraces. SAS185/P/2015 showed the highest amount of flavonoid content (3.16 ± 0.06 mg QE/g fw) followed by SAS184/G/2015 (2.68 ± 0.04 mg QE/g fw) and SAS137/P/2015 (1.91 ± 0.16 mg QE/g fw) contained the least amount of flavonoids as shown in Table 1. The total polyphenol content ranged from 3.44 ± 0.11 to 7.79 ± 0.27 mg GAE/g fw. Total polyphenol content was significantly different ($P \leq 0.05$) among the landraces with SAS1641/2015 (7.79 ± 0.27 mg GAE/g) showing the highest total polyphenol followed by SAS185/P/2015 (6.61 ± 0.15 mg GAE/g fw) and SAS145/2015 (3.44 ± 0.11 mg GAE/g fw) was observed to contain the least amount of total polyphenols as shown in Table 1.

3.2. Vitamin C

The vitamin C content as determined using UV-spectrophotometric method showed that SAS1641/2015 (1.9 ± 0.04 mg/g fw) had the highest content of vitamin C followed by SAS184/G/2015 (1.53 ± 0.15 mg/g fw) and SAS137/P/2015 (0.52 ± 0.16 mg/g fw) showed the least content of vitamin C as shown in Table 1. The results showed a significant difference ($P \leq 0.05$) in the vitamin C content among the landraces studied.

3.3. Chlorophyll content

The chlorophyll extracted using 80% acetone was determined by UV-spectrophotometer. The results showed a significant difference ($P \leq 0.05$) in the chlorophyll content of the landraces. The highest chlorophyll content was observed in SAS145/2015 (19.69 ± 0.01 mg/g dwb) followed by SAS137/P/2015 (19.54 ± 0.13 mg/g dwb) and SAS1641/2015 (17.94 ± 0.003 mg/g dwb) showed the least observed chlorophyll content.

3.4. Moisture content

High percentage moisture content was observed ranging from 82.34 ± 0.28 to $84.21 \pm 0.48\%$. The percentage moisture content of SAS148/G/2015 ($82.34 \pm 0.28\%$) was significantly different from the percentage moisture content of the other landraces except SAS1641/2015 ($82.66 \pm 0.35\%$) at $P \leq 0.05$. SAS185/P/2015 ($84.21 \pm 0.48\%$) had the highest observed percentage moisture content among all the six landraces. There was no significant difference in the percentage moisture content of the other five landraces studied as shown in Table 1.

3.5. Total antioxidant activity

The total antioxidant activity was determined using FRAP and DPPH method. The two methods showed that SAS1641/2015 had the highest total antioxidant activity of 2.79 ± 0.01 and 5.43 ± 0.02 mg AAE/g of fresh sample with FRAP and DPPH method respectively as shown in Table 2.

Table 1. Phytochemical content and moisture content of the farmer preferred landrace of *Solanum aethiopicum* Sham.

Accession number	Flav (mgQE/gfw)	T.P (mgGAE/gfw)	Total Vit. C (mg/gfw)	Chl (mg/gdwb)	Moisture %
SAS145/2015	2.30 ± 0.04^a	3.44 ± 0.11^a	1.36 ± 0.28^a	19.69 ± 0.01^a	83.49 ± 0.33^a
SAS148/G/2015	2.37 ± 0.02^b	5.04 ± 0.43^b	0.60 ± 0.02^b	19.09 ± 0.00^b	82.34 ± 0.28^b
SAS1641/2015	2.50 ± 0.09^{abc}	7.79 ± 0.27^c	1.90 ± 0.04^{ac}	17.94 ± 0.00^c	82.66 ± 0.35^{ab}
SAS185/P/2015	3.16 ± 0.06^c	6.61 ± 0.15^d	1.50 ± 0.10^{ac}	19.58 ± 0.11^a	84.21 ± 0.48^a
SAS184/G/2015	2.68 ± 0.04^c	4.38 ± 0.22^e	1.53 ± 0.15^{ac}	18.26 ± 0.03^d	83.86 ± 0.12^a
SAS137/P/2015	1.91 ± 0.16^d	4.80 ± 0.08^{be}	0.52 ± 0.16^b	19.54 ± 0.13^a	83.59 ± 0.08^a

Flav; flavonoids, DPPH; 1,1-diphenyl-2-picrylhydrazyl, FRAP; Ferric Reducing Antioxidant Power, T.P; Total Polyphenols, Total Vit C; Total Vitamin C, Chl; Chlorophyll content. Values are expressed as means \pm standard deviation. ^{abcde} Values not sharing common superscript with in a column are significantly different ($P \leq 0.05$) using Tukey HSD test.

Table 2. Total antioxidant activity determined using FRAP and DPPH method, of the farmer preferred landrace of *Solanum aethiopicum* Sham.

Landrace	Total antioxidant activity (mg AAE/g fw)	
	FRAP assay	DPPH assay
SAS145/2015	1.55±0.06 ^a	5.20±0.04 ^a
SAS148/G/2015	2.56±0.03 ^b	5.05±0.01 ^b
SAS1641/2015	2.79±0.01 ^c	5.43±0.02 ^c
SAS185/P/2015	2.66±0.03 ^{bc}	5.15±0.02 ^{ab}
SAS184/G/2015	1.53±0.08 ^a	3.84±0.07 ^d
SAS137/P/2015	1.66±0.14 ^a	4.24±0.05 ^e

Values are expressed as means ± standard deviation. ^{abcde} Values not sharing common superscript within the same column are significantly different ($P \leq 0.05$) using Tukey HSD test.

Table 3. Pearson correlation coefficient for the selected parameters and total antioxidant methods used.

Variable	DPPH	Flav	T.Ps	FRAP	Vit. C	Moisture	Chl
Flav	0.212						
T.P	0.475*	0.409					
FRAP	0.673**	0.450	0.851**				
Vit. C	0.294	0.602**	0.441	0.233			
Moisture	-0.398	0.381	-0.213	-0.400	0.194		
Chl	0.099	-0.146	-0.466	-0.260	-0.531*	0.354	
Phytates	-0.152	0.637**	0.284	0.285	-0.051	0.571*	0.294

Flav; flavonoids, DPPH; 1,1-diphenyl-2-picrylhydrazyl, FRAP; Ferric Reducing Antioxidant Power, T.Ps; Total Polyphenols, Vit. C; Vitamin C, Chl; Chlorophyll content. ** and * Correlation is significant at the 0.01 and 0.05 level respectively.

This high total antioxidant activity may have been due to the high total polyphenol, flavonoid and vitamin C content as shown in Table 1. The lowest total antioxidant activity was observed in SAS184/G/2015 (1.53±0.08 and 3.84±0.07 mg AAE/g of fresh sample with FRAP and DPPH methods respectively).

4. DISCUSSION

The phytochemical content of vegetables is determined by the presence and activation of key enzymes for example phenylalanine ammonia-lyase, γ -tocopherol methyltransferase, l-galactose dehydrogenase which are responsible for the biosynthesis of polyphenols, α -tocopherol, and ascorbic acid respectively [17, 18]. The significant difference in the phytochemical attributes and moisture content of

the landraces of *Solanum aethiopicum* is attributed to the genetic differences in the respective landraces [19]. The high antioxidant activity of SAS1641/2015 is due to its high flavonoid, total polyphenol and vitamin C content as shown in Table 1. This is explained by the positive correlation of flavonoid content, total polyphenol content and vitamin C content showed with the total antioxidant activity when determined using both FRAP and DPPH methods. This positive correlation is previously demonstrated by other researchers [20]. The high total antioxidant activity was mainly contributed by the polyphenols as shown in Table 3, as total polyphenols have significant correlation at 0.01 level with total antioxidant activity determined using FRAP method and with that when using DPPH method at 0.05 level. *Solanum aethiopicum* is a green leafy vegetable with high moisture content

as results show in Table 1. This has also been shown in other studies done earlier on indigenous vegetables [21-24]. The high chlorophyll content of all the landraces increases the acceptability of this vegetable since this depends on appearance and texture [7].

5. CONCLUSION

The present research provides for the first time a report on the phytochemical qualities and antioxidant activity of selected landraces of *S. aethiopicum* preferred by farmers. All *S. aethiopicum* landraces studied had a high content of polyphenols and antioxidant activity. This makes *S. aethiopicum* an important plant for the control of diseases like cancer, diabetes mellitus and heart diseases. Ugandans should be encouraged to consume these vegetable in order to avert oxidative stress related diseases. The high percentage moisture content of *S. aethiopicum* explains its short shelf life and calls for a proper storage technology if it is to be consumed fresh. Within the landraces are physiological and biochemical differences that result in differences in phytochemical content. There is need therefore for a study on the genetic differences of the different landraces of *S. aethiopicum* and how the genetics affects the phytochemical content and shelf life of the landraces and also develop a storage technology that can preserve the chlorophyll content and regulate the yellowing effect of ethylene.

ACKNOWLEDGEMENT

The following are acknowledged, Makerere University School of Food Technology, Nutrition and Bio-engineering system for the research facilities, financial support provided by EU (PAEPARD/CRFII) through FARA and Uganda Christian University.

AUTHOR'S CONTRIBUTION

SS: Developing and designing the concept, developing the methodology, collecting, analysis and interpretation of data and writing, review and revision of the manuscript. A Nandutu: Involved in the developing, designing the concept, developing the methodology, analysis and interpretation of data, provided technical support and involved in the study supervision, review and revision of the manuscript. A Namutebi: Developing and designing

the concept, developing the methodology, analysis and interpretation of data, provided administrative, technical and material support, involved in the study supervision. JS: involved in acquisition of data and administration. EBK: was involved in the development and design of the concept, screening of the landraces and provided administrative, technical and material support. PK: Involved in the screening of the landraces, development of the concept and acquisition of data. JNJ: Involved in the administration of the project. AK: Involved in the screening of the landraces, provided administrative and technical support. DR: Provided administrative and material support. The final manuscript has been approved by all authors.

TRANSPARENCY DECLARATION

The authors declare that there is no conflict of interest regarding the publication of this article.

REFERENCES

1. Garcia-Salas P, Patricia M, Aranzazu S, Antonio FA. Phenolic-compound-extraction systems for fruit and vegetable samples. *Molecules*. 2010; 15(12): 8813-8826.
2. Valko M, Leibfritz D, Moncol J, Cronin MTD, Mazur M, Telser J. Free radicals and antioxidants in normal physiological functions and human disease. *Int J Biochem Cell Biol*. 2007; 39(1): 44-84.
3. Ssekabembe C, Bukenya C, Nakyagaba W. Traditional knowledge and practices in local vegetable production in central Uganda. *Afr Crop Sci Conf Proc*. 2003; 6: 14-19.
4. Slavin JL, Lloyd B. Health benefits of fruits and vegetables. *Adv Nutr Int Rev J*. 2012; 3(4): 506-516.
5. Prabhu S, Barrett DM. Effects of storage condition and domestic cooking on the quality and nutrient content of African leafy vegetables (*Cassia tora* and *Corchorus tridens*). *J Sci Food Agricult*. 2009; 89(10): 1709-1721.
6. Chinedu SN, Olasumbo AC, Eboji OK, Emiloju OC, Orinola OK, Dania DI. Proximate and phytochemical analyses of *Solanum aethiopicum* L. and *Solanum macrocarpon* L. fruits. *Res J Chem Sci*. 2011; 1(3): 63-71.
7. Toivonen PM, Brummell DA. Biochemical bases of appearance and texture changes in fresh-cut fruit and vegetables. *Postharv Biol Technol*. 2008; 48(1): 1-14.
8. Wissam Z, Ghada B, Wissam A, Warid K. Effective extraction of polyphenols and proanthocyanidins

- from pomegranate's peel. *Int J Pharm Pharm Sci*. 2012; 4(Suppl. 3): 675-682.
9. Demiray S, Pintado M, Castro P. Evaluation of phenolic profiles and antioxidant activities of Turkish medicinal plants: *Tilia argentea*, *Crataegi folium* leaves and *Polygonum bistorta* roots. *World Acad Sci Engin Technol*. 2009; 54(30): 312-317.
 10. Majhenič L, Škerget M, Knez Ž. Antioxidant and antimicrobial activity of guarana seed extracts. *Food Chem*. 2007; 104(3): 1258-1268.
 11. El Far MM, Taie HA. Antioxidant activities, total anthocyanins, phenolics and flavonoids contents of some sweetpotato genotypes under stress of different concentrations of sucrose and sorbitol. *Austr J Basic Appl Sci*. 2009; 3(4): 3609-3616.
 12. Braca A, De Tommasi M, Di Bar L, Pizza C, Politi M, Morelli I. Antioxidant principles from *baubinia tarapotensis*. *J Nat Prod*. 2001; 64(7): 892-895.
 13. Iqbal E, Salim KA, Lim LB. Phytochemical screening, total phenolics and antioxidant activities of bark and leaf extracts of *Goniothalamus velutinus* (Airy Shaw) from Brunei Darussalam. *J King Saud Univ Sci*. 2015; 27(3): 224-232.
 14. Mohammed QY, Hamad WM, Mohammed EK. Spectrophotometric determination of total vitamin C in some fruits and vegetables at Koya Area - Kurdistan Region/Iraq. *J Kirkuk Univ Sci Stud*. 2009; 4(2): 46-54.
 15. Straumite E, Kruma Z, Galoburda R. Pigments in mint leaves and stems. *Agron Res*. 2015; 13(4): 1104-1111.
 16. AOAC. Official Methods of Analysis of the Association of Official Analytical Chemists. AOAC: Arlington, Virginia, 1995.
 17. Moskaug JØ, Carlsen H, Myhrstad MC, Blomhoff R. Polyphenols and glutathione synthesis regulation. *Am J Clin Nutr*. 2005; 81(1): 277S-283S.
 18. Oh M-M, Carey EE, Rajashekar C. Environmental stresses induce health-promoting phytochemicals in lettuce. *Plant Physiol Biochem*. 2009; 47(7): 578-583.
 19. Schijlen EG, De Vos CR, van Tunen AJ, Bovy AG. Modification of flavonoid biosynthesis in crop plants. *Phytochem*. 2004; 65(19): 2631-2648.
 20. Olajire A, Azeez L. Total antioxidant activity, phenolic, flavonoid and ascorbic acid contents of Nigerian vegetables. *Afr J Food Sci Technol*. 2011; 2(2): 22-29.
 21. Gupta S, Lakshmi AJ, Manjunath M, Prakash J. Analysis of nutrient and antinutrient content of underutilized green leafy vegetables. *LWT Food Sci Technol*. 2005; 38(4): 339-345.
 22. Nnamani C, Oselebe H, Agbatutu A. Assessment of nutritional values of three underutilized indigenous leafy vegetables of Ebonyi State, Nigeria. *Afr J Biotechnol*. 2009; 8(9): 2321-2324.
 23. Odhav B, Beekrum S, Akula U, Baijnath. Preliminary assessment of nutritional value of traditional leafy vegetables in KwaZulu-Natal, South Africa. *J Food Comp Anal*. 2007; 20(5): 430-435.
 24. Singh G, Kawatra A, Sehgal S. Nutritional composition of selected green leafy vegetables, herbs and carrots. *Plant Foods Human Nutr*. 2001; 56(4): 359-364.

Comparative stem anatomy of four taxa of Calycanthaceae Lindl.

Niroj Paudel, Kweon Heo*

Division of Biological Resource Sciences, Kangwon National University, Chuncheon, 24341, South Korea

*Corresponding author: Kweon Heo; Phone: +82-33-250-6412; E-mail: laurus@kangwon.ac.kr

Received: 15 January 2018; Revised submission: 09 March 2018; Accepted: 14 March 2018

Copyright: © The Author(s) 2018. European Journal of Biological Research © T.M.Karpiński 2018. This is an open access article licensed under the terms of the Creative Commons Attribution Non-Commercial 4.0 International License, which permits unrestricted, non-commercial use, distribution and reproduction in any medium, provided the work is properly cited.

DOI: <http://dx.doi.org/10.5281/zenodo.1199578>

ABSTRACT

The anatomical character is potential value in Calycanthaceae for their taxonomic study. Four species of Calycanthaceae were collected for this experiment. The experiment was done using the resin methods for preparation of the permanent slide for anatomical studies. The anatomical character like two traces of the unilocular vascular bundle, in the primary vascular cylinder, contains four cortical vascular bundles in the stem, the unilocular structure of primary cylinder, the presence of numerous intercellular space in phloem, the presence of oil cell in the form of scatter in *Calycanthus* whereas small size in *Chimonanthus*. *Calycanthus* possess boarder pit with circular aperture while *Chimonanthus* possess elliptical. The tracheid is a characteristic feature of the spiral band wider in *Chimonanthus* than that of *Calycanthus* and *Sinocalycanthus*. The noted sclerenchymatous cells are grouped of the colony which is a characteristic feature of *Sinocalycanthus* and *Calycanthus* but in case of *Chimonanthus* is the long chain with the layer of the cell. Collenchymatous cell was circular with an intercellular in *Calycanthus*; ovoid shape with the intercellular in *Chimonanthus* but in *Sinocalycanthus* is elongation with the minor regular shape. The different character of pith cells found in hexagonal and circular shape which is also distinguished feature in Calycanthaceae. The valu-

able stem anatomical characters are the importance of their function, ontogeny, and phylogeny.

Keywords: Anatomical character; Calycanthaceae; Collenchyma; Sclerenchymatous; Vascular bundle.

1. INTRODUCTION

Calycanthus, *Chimonanthus*, and *Sinocalycanthus* are the genus of Calycanthaceae. *Sinocalycanthus* is native to China. *Sinocalycanthus* is the synonym of *Calycanthus*. The literature reveals that long horticulture forms and varieties due to the long cultivation of history. Calycanthaceae is the small family of the plant with four genera and ten species which is the sister group of Laurales [1-7]. Within Calycanthaceae, the deepest split is between the tropical monotypic tree *Idiospermum australiense* and the temperate shrubs of the rest of the family Calycanthoideae (Calycanthaceae) [8, 9], unique in Laurales are features of the gynoecium: ovule number and placentation differ from all other Laurales, and the seeds in *Idiospermum* have the largest embryos known in angiosperms [5, 10]. Although very old Chinese drawings and Japanese wood figures of *Chimonanthus* are apparently in existence [11], the first drawing to appear in the taxonomic literature was probably that [12, 13]. *Calycanthus floridus* Linneaus [14] recognized only the genus *Calycanthus* with the two species

Calycanthus floridus and *Calycanthus praecox* [13], as well as Lindley [11], considered *Calycanthus praecox* to represent a new genus *Chimonanthus*. Some authors [13, 15, 16] maintained this concept of two genera. Others [18, 19] followed Linnaeus in recognizing only one genus. Prantl [18], the other hand, recognized two sections, viz., *Eucalycanthus* and *Chimonanthus*. There has been some confusion in the past concerning the correct names for these genera. However, the designation of *Calycanthus* L. and *Chimonanthus* Lindley as nomina conservanda Lanjouwa [19] has solved this problem. The pertinent nomenclatural information and synonymy have been summarized by Kearney [20] and Rehder [21] for *Calycanthus* and by Rehder and Wilson [13] for *Chimonanthus*. *Chimonanthus* was monotypic until the description of *Chimonanthus nitens* by Oliver [22] based on material from August Henry's collections from central China. With more complete collections, two additional species have been proposed, *Chimonanthus yunnanensis* Smith [23] and *Chimonanthus salcifolius* Hu [24]. The situation is somewhat different in *Calycanthus*. Although *C. occidentalis* of California has been recognized as comprising a distinct and relatively uniform species, the plants of the southeastern United States have been treated as representing from one to as many as six species. Rafinesque [25] represented the latter extreme by stating to the sp. of *Calycanthus* L. only one. In most manuals at least two species *C. floridus*

and *C. fertilis* have been recognized based primarily differences in pubescence and leaf shape.

The aim of this study is the histological comparison of the stem of Calycanthaceae for the purpose of discussion and implication of observed anatomical trait for support the classification of the plant.

2. MATERIAL AND METHODS

Altogether four species (Table 1) is collected. The stems were fixed with the FAA (formalin: glacial acetic acid: 50% ethanol, 5:5:90, by volume) from each family mature stem were selected then passed alcohol series after that; alcohol: technovit 7100 resin. Serial section of 5-6 μm thickness was cut using disposable blade knives stuck into glass slides and dried on electrical slide hot plate for Twenty four hour; slides were stained with 0.1% toluidine blue for 60-90 second. After that rinsed with running water, and again dried on the electric hotplate for more than six hours to remove water. The stained slides were then the mounted with Entellen. Four permanent slides were observed under an Olympus BX-50 light microscope (Olympus Co. Japan), Photographs were taken with the digital camera system attached to the microscope and multiple image alignment was done using Photoshop.

Table 1. Collection information of genus and species used in the present study.

Taxa	Collection information
<i>Calycanthus occidentalis</i> Hook. & Arn.	Korea, Cultivated at Kangwon University, K. Heo & N. Paudel s.n. 2016 (KWNU)
<i>Chimonanthus praecox</i> Lindl.	Korea, Cultivated at Kangwon University, K. Heo & N. Paudel s.n. 2016 (KWNU)
<i>Chimonanthus salcifolius</i> S.Y. Hu	Korea, Cultivated in Chollipo Arboritum, K. Heo s.n. 2009
<i>Sinocalycanthus chinensis</i> W.C. Cheng & S.Y. Chang	Korea, Cultivated at Kangwon University, K. Heo & N. Paudel s.n. 2016 (KWNU)

3. RESULTS

Epidermis the single-layered outermost composed of tabular parenchyma cells (Table 2) which are compactly arranged without having inter-cellular

spaces in *Chimonanthus praecox* (fig. 2C) and *Chimonanthus salcifolius* (fig. 2C). In *Sinocalycanthus chinensis* and *Calycanthus occidentalis* were intercellular space in the epidermal cell (figs. 1C, 2I). Outer walls were cuticularised. Collen-

chymatous cells are a circular shape which is interconnected with each other layer in *Chimonanthus praecox* and *Chimonanthus salcifolius* (figs. 1I, 2I). Sclerenchymatous cells are higher cell grouped in *Sinocalycanthus chinensis* and *Calycanthus occidentalis* whereas in *Chimonanthus praecox*, and *Chimonanthus salcifolius* formation of long 2 layer chain (figs. 1I, 1D) with two traces of unilocular vascular system was noted in all species *Sinocalycanthus chinensis*, *Calycanthus occidentalis*, *Chimonanthus praecox*, and *Chimonanthus salcifolius*. In primary vascular cylinder, four cortical vascular bundles were noted in all species in Calycanthaceae (figs. 1A, 1G, 2A, 2G). A cortical bundle which is later developed in the central bundle in the stem. Especially unilocular system is in the primary vascular cylinder in all species (figs. 1D, 2H, 2C, 2I). *Calycanthus occidentalis* has circular border pits (fig. 1E). In the center, pith is a loosely bound hexagonal structure (fig. 1F) with intercellular. Parenchymatous cell are in circular and ovoid shaped whereas sclerenchymatous cells are in group colony contains thirteen number of cells (fig.1D) Protoxylem vessels with wider cavities with

annular thickening towards the epidermal cell (figs. 1G, 1H). Pentagonal intercellular space gap was seen in *Calycanthus occidentalis* (fig 1I). The tracheid possesses spiral band (figs.1E, 1K).

Chimonanthus praecox possess straight chain border pits which are undergoing towards the epidermis (fig.1K) with elliptical aperture. The pith cell circular with intercellular space was noted in *Chimonanthus praecox* (fig. 1L). The parenchymatous cells were rectangular in shape possess the large intercellular space (figs. 1I, 1J).

Chimonanthus salcifolius also possess straight chain bordered pits (fig. 2E). Parenchymatous cells are circular or ovoid shaped with intercellular space (figs. 2C, 2D) the vascular bundle is collateral (figs. 2B) the pith cell are also noted large circular cell with intercellular space (figs. 1L, 2F).

Sinocalycanthus chinensis parenchymatous cells are ovoid with some rectangular shape (figs. 2I, 2J). The vascular bundle is noted four in each quadrangular side (fig. 2G). The cortical bundle is also the lateral side of the stem (fig. 2H). The pitch cells are large with intercellular space with circular as well as hexagonal shape (fig. 2L).

Table 2. Comparative stem anatomical characters of Calycanthaceae.

Taxa	Epidermis	Collenchyma	Parenchyma	Sclerenchyma	Endodermis	Number of vascular bundle	Xylem	Pith
<i>Calycanthus occidentalis</i> Hook.& Arn.	Single layered	Circular shape, loosely bind	Ovoid or circular shape	13-14 cells in the group, scatter	Single layered, parenchymatous cell	4	Protoxylem vessels with wider cavities	Hexagonal shape with intercellular space, loosely bind each other
<i>Chimonanthus praecox</i> Lindl.	Single layered	Ovoid shape, intercellular space	circular shape	2-6 cells in the group, scatter	Single layered, parenchymatous cell	4	Protoxylem vessels with smaller cavities	Circular shape, loosely bind
<i>Chimonanthus salcifolius</i> S.Y. Hu	Single layered	Ovoid shape, intercellular space	Circular shape	2-7 cells in the group, scatter	Single layered, parenchymatous cell	4	Protoxylem vessel with smaller cavities	Circular shape
<i>Sinocalycanthus chinensis</i> W.C. Cheng & S.Y.Chang	Single layered	Elongation shape, intercellular space	Ovoid or elongation shape	14-17 cells in a group, scatter	Single layered, parenchymatous cell	4	Protoxylem vessel with wider cavities	Hexagonal shape interact with each other

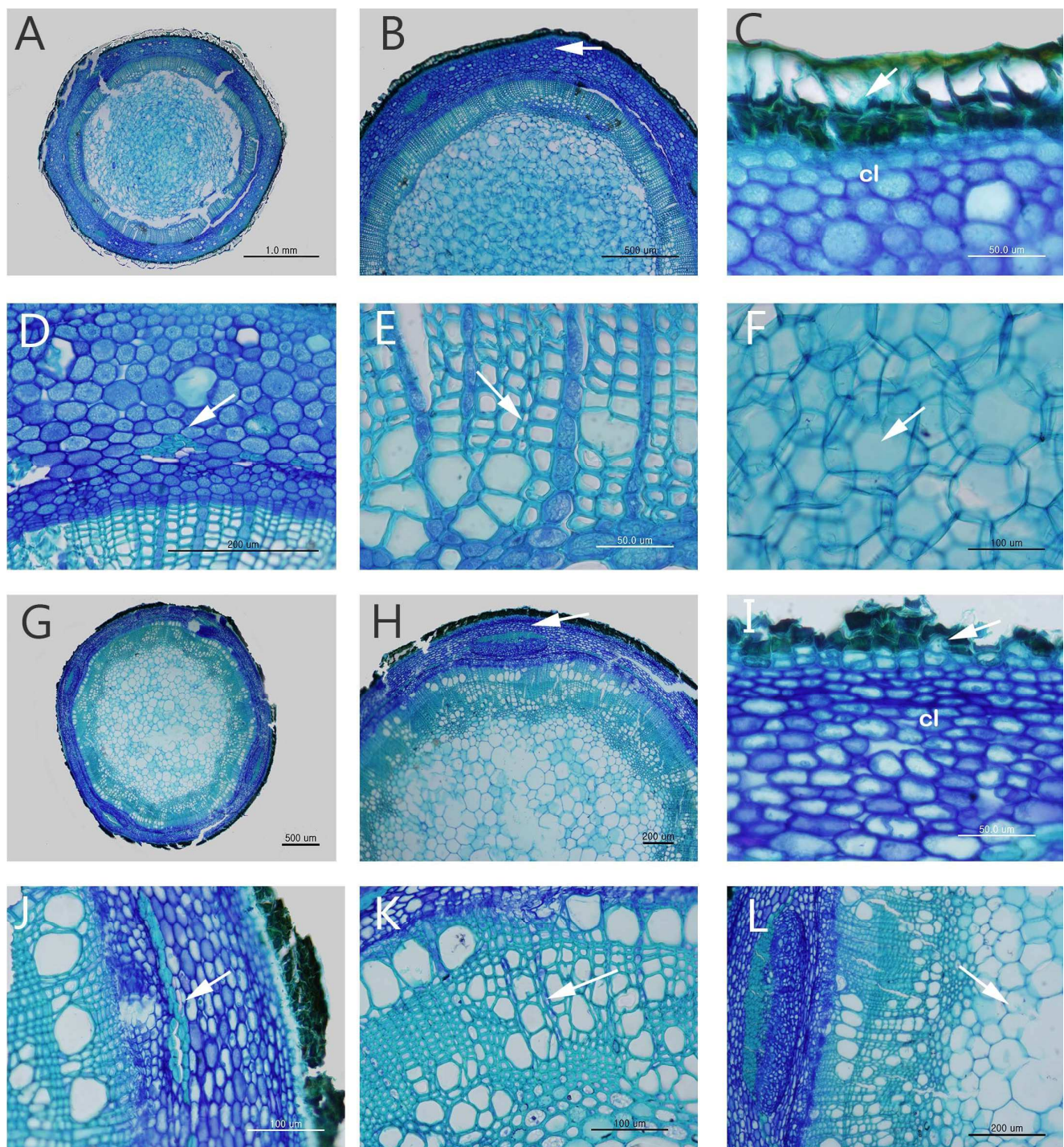


Figure 1. *Calycanthus occidentalis* (A-F); **A.** Cross section of young stem, **B.** A detail portion of cross section (arrow head shows the vascular bundle), **C.** Epidermis and collenchyma (arrow head represent epidermis, and cl shows collenchyma), **D.** Sclerenchyma with the colony, **E.** Tracheid and vessel, **F.** Pith. *Chimonanthus praecox* (G-H); **G.** Cross section of young stem, **H.** A detail portion of cross section (arrow head shows the vascular bundle), **I.** Epidermis and collenchyma (arrow head represents epidermis, and cl shows collenchyma), **J.** Sclerenchyma with the colony, **K.** Tracheid and vessel, **L.** Pith.

4. DISCUSSION

The stem of the Calycanthaceae is characterized by its quadrangular appearance (figs. 1A, 1H, 2A, 2G). This is usually quite in young stems but

less in older ones. The tissues of the mature stem have received a close examination by several researchers. Much of the research has focus on the presence of inverted cortical bundles in the stem.

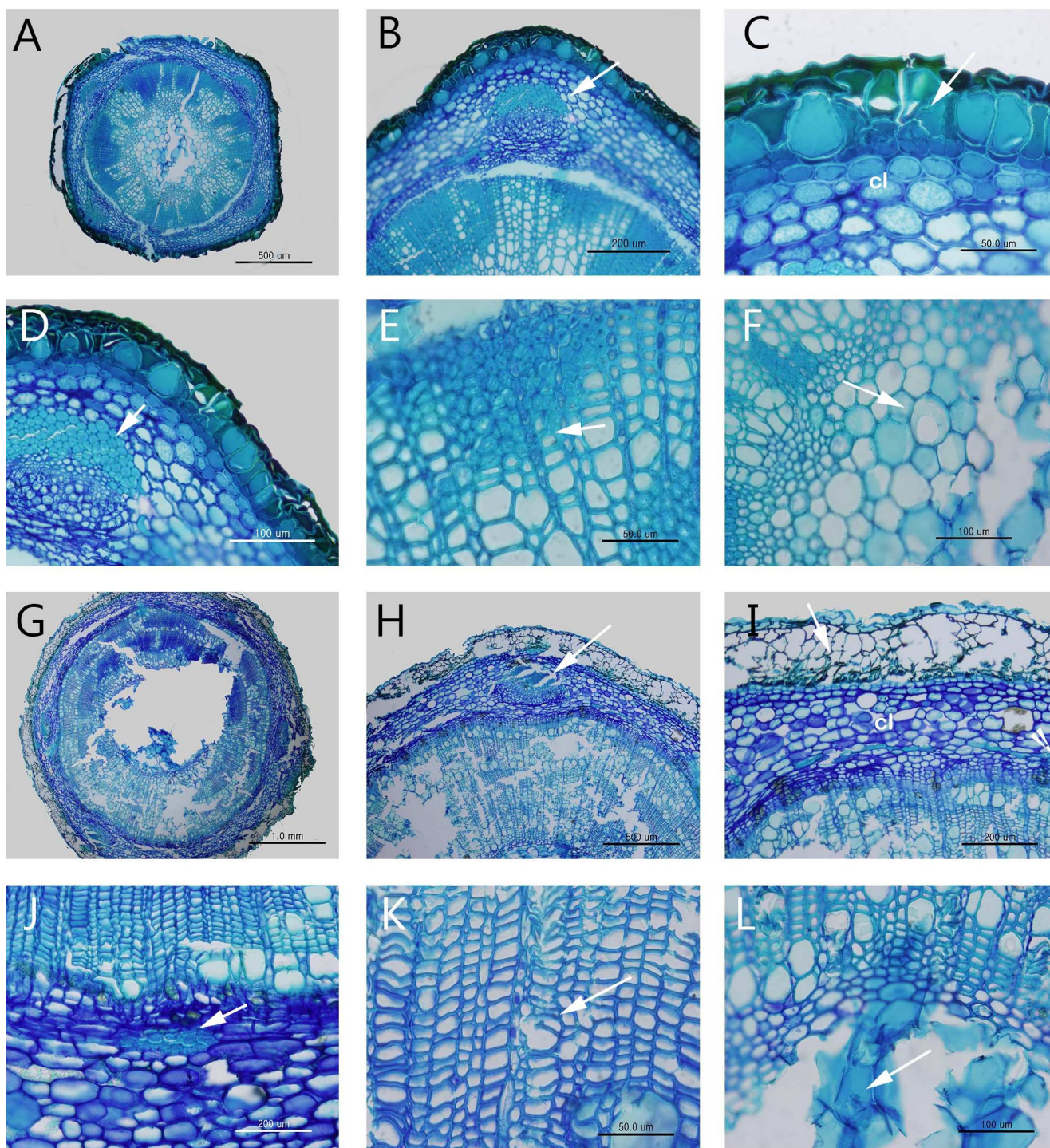


Figure 2. *Chimonanthus salcifolius* (A-F); **A.** Cross section of young stem, **B.** A detail portion of cross section (arrow head shows the vascular bundle), **C.** Epidermis and collenchyma (arrow head represent epidermis, and cl shows collenchyma), **D.** Sclerenchyma with colony, **E.** Tracheid and vessel, **F.** Pith; *Sinocalycanthus chinensis* (G-L); **G.** Cross section of young stem, **H.** A detail portion of cross section (arrow head shows the vascular bundle), **I.** Epidermis and collenchyma (arrow head represent epidermis, and cl shows collenchyma), **J.** Sclerenchyma with colony, **K.** Tracheid and vessel, **L.** Pith.

The literature has been summarized by Metcalf and Chalk [26], Solereder [27] and in part by Bennett [28] and Quinlan [29]. Quinlan [29] found only slight differences between members of the family. The more important of these works are summarized

in the following treatment. The work concerning the vascular system of the family is that of Fahn and Bailey [30] who studied the nodal anatomy of both *Calycanthus* and *Chimonanthus*. They found the family to possess a two-trace, unilacunar vascular

system. Such a nodal structure is now recognized to be primitive among angiosperms and also occurs in the Austrobaileyaceae, Monimiaceae, Annonaceae and Winteraceae among others [31]. They have noted some differences between species of Calycanthaceae in the level of branching and fusion of the vascular bundles of the eustele. This could be utilized as a taxonomic feature which is also supported by our results. In addition to the primary vascular cylinder, four cortical vascular bundles occur in the stem. These were first described [29] and have long drawn the attention of plant anatomists. There has been some disagreement as to their origin and phylogenetic significance and the various descriptions and viewpoints have been summarized by [28] and [29] in a detailed study of the seedling, stated: "Cortical bundles were found to originate from the primary vascular poles of the root after they had diverged from the central cylinder to become the trace to the cotyledon. This is the only point at which the cortical system connects with the central style of the stem. Fahn and Bailey [30] in general agreed with the observations of Bennett. In their study of the eustele as well as the cortical system of the mature stem and seedlings, they found no evidence that the cortical system is a modification of lateral traces of a trilacunar or multilacunar nodal system, as is the apparent case in some dicot families [31], but believed that it is an additional independent system which has been superimposed upon the double trace, unilacunar structure of the primary cylinder. They also indicated that transverse connections between the cortical strands which are present in the nodal region of *Calycanthus* are less well developed in *Chimonanthus*."

A complete and detailed description of the phloem of the Calycanthaceae has been given by Cheadle and Esau [32]. Our results also show *Calycanthus occidentalis*, *Chimonanthus praecox*, *Chimonanthus salcifolius* and *Sinocalycanthus chinensis* in which they found the phloem to be very similar and to possess the following characteristics in common: absence of fibers, sclereids, the presence of numerous intercellular spaces, presence of oil cells in varying degrees of abundance, uniseriate to multiseriate rays, sieve elements with thick nacreous walls, and simple sieve plates located laterally or on the end walls in an oblique or

transverse manner. Oil cells were found to be in *Calycanthus occidentalis*, and infrequent and usually smaller in *Chimonanthus praecox*, whereas *Chimonanthus salcifolius* and *Sinocalycanthus chinensis* possess big size. In *Sinocalycanthus chinensis* we also demonstrated a more irregular cell pattern with sieve tubes in more markedly isolated strands than in either *Calycanthus occidentalis* or *Chimonanthus praecox* and *Chimonanthus salcifolius*. Characteristics of the secondary wood of the family have been summarized by Metcalf and Chalk [26]. Lemesle [33] in his rather extensive study, reported differences primarily between the two genera in tracheid characteristics.

Those of *Calycanthus* and *Sinocalycanthus* possess bordered pits with circular apertures while those of *Chimonanthus* possess more elliptical apertures. Lemesle [33] considered the wood of *Calycanthus* to be more primitive, at least in this characteristic. Tracheids are quadrangular in cross section. The internal surface of the tracheids possesses spiral bands which are stated to be slightly wider in *Chimonanthus* than in *Calycanthus*. We also supported that the majority of the tracheids possess simple oval or oblong perforations although some tracheids may be devoid of the connecting perforations. The vessels are small, polygonal in cross section and possess simple perforations. The fibers are libriform and almost completely devoid of bordered pits in Calycanthaceae.

There was no detail character for the stem in Calycanthaceae. Sclerenchyma possesses chain and colony structure which is a new character for young stem anatomy in Calycanthaceae.

Key to the genera of Calycanthaceae based on the stem anatomy:

1. Sclerenchyma is (14-17) cells group formation of the colony, protoxylem vessel is wider cavity *Sinocalycanthus*
2. Sclerenchyma is (13-14) cells group formation of colony, protoxylem vessel is wider cavity *Calycanthus*
3. Sclerenchyma is arranged in the long chain with two layers, protoxylem vessel is smaller cavity *Chimonanthus*

AUTHOR'S CONTRIBUTION

Both authors have equal contribution. KH: supervisor, research design; sample collection; NP: research design; sample collection, experimental design. All authors have approved the final manuscript.

ACKNOWLEDGMENT

We would like to thank for the department of applied plant science Kangwon National University (KNU) for laboratory facilities and, also thanks for the study supported by 2016 research grant from KNU (No. 5201160225).

TRANSPARENCY DECLARATION

The authors declare that there is no conflict of interest regarding the publication of this article.

REFERENCES

- Garcia-Salas P, Patricia M, Aranzazu S, Antonio L, Renner SS. Circumscription and phylogeny of the Laurales: evidence from molecular and morphological data. *Am J Bot.* 1999; 86: 1301-1315.
- Renner SS. Variation in diversity among Laurales, Early Cretaceous to present. *Biologiske Skrifter/ Kongelige Danske Videnskabernes Selskab.* 2005; 55: 441-458.
- Cheng WC, Chang SY. Genus novum *Calycanthacearum chinaeorientalis*. *Acta Phytotax Sin.* 1964; 9: 137-138.
- Nicely KA. A monographic study of the Calycanthaceae. *Castanea.* 1965: 38-81.
- Blake ST. *Idiospermum* (Idiospermaceae), a new genus and family for *Calycanthus australiensis*. *Contrib Queensland Herb.* 1972; 12: 1-37.
- Jin ZX, Li JM. ISSR analysis on genetic diversity of endangered relic shrub *Sinocalycanthus chinensis*. *J Appl Ecol.* 2007; 18(2): 247-253.
- YM, Weston PH, Endress PK. Floral phyllotaxis and floral architecture in Calycanthaceae (Laurales). *Int J Plant Sci.* 2007: 168: 285-306.
- Li J, Ledger J, Ward T, Del TP. Phylogenetics of Calycanthaceae based on molecular and morphological data, with a special reference to divergent paralogues of the nrDNA ITS region. *Harvard Papers Bot.* 2004: 69-82.
- Zhou S, Renner SS, Wen J. Molecular phylogeny and intra- and intercontinental biogeography of Calycanthaceae. *Mol Phylogen Evol.* 2006; 1: 1-15.
- Endress PK. Dispersal and distribution in some small archaic relic angiosperm families (Austrobaileya-ceae, Eupomatiaceae, Himantandraceae, Idiospermoideae, Calycanthaceae). *Sonderbd Naturwiss Ver Hamburg.* 1983; 7: 201-217.
- Lindley J. *Edwards' Botan Reg.* 1819; 5: 404.
- Curtis S. *Curtis' Botan Mag.* 1799; 13: 466.
- Rehder A, Wilson EH. In Sargent, *Plantae Wilsonianae*; 1913; 1: 419420.
- Linneus. *C Syst. Nat. ed.* 1759; 10(2): 1066.
- Candolle AP. *Prodromus systematis naturalis regni vegetabilis.* Paris. 1828; 3: 1-2.
- Bentham G, Hooker JD. *Genera plantarum.* Reeve and Company, London. 1862; 1: 16.
- Willdenow KL. *Enumeratio plantarum horti botanici Berolinensis.* Berlin. 1809: 559.
- Prant K. *Naturl. Pflfam.* 1888; III(2): 94.
- Lanjouw J. *International code of botanical nomenclature.* Utrecht, Netherlands, 1961.
- Kearney T. The nomenclature of the genus *Buttneria* Duham. *Bull Torrey Botan. Club.* 1894.
- Rehder A. *Bibliography of cultivated trees and shrubs.* Arnold Arboretum, Harvard Univ. 1949: 185-187.
- Oliver D. In Hooker, *Icon. Plant.* 1887; 16: 1600.
- Smith GH. Vascular anatomy of Ranalian flowers II. Ranunculaceae (Cont.), Menispermaceae, Calycanthaceae, Annonaceae. *Botan Gaz.* 1928; 85: 152-177.
- Hu SY. A monograph of the genus *Philadelphus*. *J Arnold Arboretum.* 1954; 35(4): 275-333.
- Raifinesque CS. *Asograpia American.* Philadelphia. 1838: 6-9.
- Metcalfe CR, Chalk L. *Anatomy of the dicotyledons.* Clarendon Press, Oxford. 1950; 1: 13-16.
- Solereder. *Systematic anatomy of dicots.* Clarendon press, Oxford. 1908; 1: 25-27.
- Bennett HD. Some aspects of the seed and seedling anatomy of *Calycanthus floridus* L. *Doctoral dissertation, State University of Iowa,* 1950.
- Quinlan CE. Contributions toward a knowledge of the lower dicotyledons III. The anatomy of the stem of the Calycanthaceae. *Trans Roy Soc Edinb.* 1920; 52: 517-530.

30. Fahn A, Bailey IW. The nodal anatomy and primary vascular cylinder of the Calycanthaceae. *J Arnold Arbor.* 1957; 38: 107-117.
31. Eames AJ. *Morphology of the angiosperms.* 1st edn., 1961.
32. Cheadle VI, Esau K. Secondary phloem of Calycanthaceae. *Univ Calif Publ Bot.* 1958; 29: 397-510.
33. Lemesle R. Tracheides a ponctuations areolees a ouvertures circulaires dans le genre *Calycanthus*. *Compt Rend Acad Sci Paris.* 1947; 225: 761-763.